



**Politecnico
di Torino**

Politecnico di Torino

Master's Degree in Geo-Engineering

a.y. 2021/2022

**3D AND 2D NUMERICAL MODELS OF MECHANISED
EXCAVATION OF OVERLAPPED TUNNELS IN URBAN
AREA: SENSITIVITY ANALYSIS FOR THE EVALUATION
OF INDUCED SETTLEMENTS AND BUILDING DAMAGE
VARYING THE EXCAVATION SEQUENCE**

Supervisors:

Prof. Daniele PEILA

Eng. Michele PALOMBA (Systra SWS)

Candidate:

Pietro Tremaggi

INDEX

INTRODUCTION	1
1. GENERAL DESCRIPTION OF THE PROJECT	3
1.1. Geological and hydrogeological data	6
1.2. Earth Pressure Balance:	7
2. SETTLEMENT INDUCED BY SINGLE AND TWIN TUNNELS	16
2.1. Shape of the zone of influence.....	20
2.2. Evaluation of the surface settlement	21
2.2.1. Empirical method	22
2.2.2. Semi-empirical method.....	23
2.2.3. Analytical method.....	24
2.2.4. Numerical method.....	26
2.3. Twin tunnels	29
3. BUILDING INDUCED DAMAGE	35
3.1. Building Condition Survey (BCS)	37
3.2. Building Risk Assessment (BRA).....	38
4. THREE-DIMENSIONAL FEM ANALYSIS WITH MIDAS FEA NX	47
4.1. Geological and geotechnical characterization of the site	47
4.2. Creation of 3D geometry.....	50
4.3. Mesh generation.....	52
4.4. Static Analysis	57
4.4.1. Static conditions input	57

4.4.2. Load condition and its calculation.....	58
4.5. Stage Wizard	61
5. TWO-DIMENSIONAL FEM ANALYSIS WITH PLAXIS 2D.....	65
5.1. Geometry of the model and mesh generation	65
5.2. Staged construction	69
5.2.1. Construction Stages with the three different alignments	70
5.2.2. Construction Stages with vertical alignment.....	70
6. RESULTS AND INTERPRETATIONS	73
6.1. Three-dimensional numerical analysis	73
6.2. Two-dimensional analysis: worst arrangement.....	75
6.3. Two-dimensional analysis: piggyback tunnels	80
6.3.1. Best construction sequence and pressure combination.....	81
6.3.2. Induced damage on the buildings	85
7. CONCLUSIONS	94
ACKNOWLEDGEMENTS	97
BIBLIOGRAPHY	98
FIGURE INDEX	101
TABLE INDEX	103

INTRODUCTION

In the world, the increasing need of the improvement of the transportation infrastructures led to a raise of the excavation in the subsurface, especially urban for tunnelling. Assessing the tunnel-induced settlements is the main issue for the prediction of the ground movements and associated risk to the surrounding buildings. The problem become more complex in presence of the twin tunnel excavation. For this reason, the aim of this thesis is to analyse the in term of induced settlements and building damage risk the excavation of two overlapped tunnels varying the construction sequence.

The thesis focuses on the project of the metro M5 of Bucharest, realised in order to improve the underground network with the aim to reduce the congestion on the surface. This new metro line is characterised by two twin tunnels, which change their relative position along the alignment. Most of the arrangement is in horizontal configuration, however approaching the stations, it becomes offset and then piggyback. The excavation of the tunnels is realised with an Earth Pressure Balance machine.

The study evaluates the induced ground surface settlement changing the construction process and the layout of the two tunnels. This aim is fulfilled by numerical FEM analysis in three and two dimensions. The 3D numerical model is realised with the software MIDAS FEA NX, which is able to simulate the three-dimensional effects of the excavation. Moreover, the 2D numerical model is developed with the software PLAXIS 2D due to its simplicity in order to cross-check the three-dimensional outputs.

In addition, a sensitivity analysis to detect the induced damage to the building is designed.

As first in the **chapter 2**, the problem of the ground surface settlement induced by the tunnelling excavation is presented, highlighting some theories to describe it. Moreover, an equation to calculate the settlement related to the excavation of twin tunnels, taking into account the mutual effect between them, is defined.

In the **chapter 3**, the sensitivity analysis is described focusing on the two main steps: the Building Condition Survey (BCS) and the Building Risk Assessment (BRA).

The 3D numerical simulations are treated in the **chapter 4**, in which the main steps able to correct design a 3D model is presented. The 3D model allows the most accurate representation of the reality; in particular the excavation process, taking into account the passage of the shield, the installation of the segmental lining and the injection of the grout.

Furthermore, in the **chapter 5** there is the description of the 2D model. Two main analyses are conducted: the assessment of the worst tunnels arrangement and the evaluation of the induced settlements under a building foundation.

Finally, the **chapter 6** presents the results of the analysis and their interpretation.

1. GENERAL DESCRIPTION OF THE PROJECT

The development of Bucharest city in the recent years is caused by huge concentration of population and the economic activities together with the importance of the city being the capital of Romania. For these reasons, the city requires an extensive infrastructures fulfilment to response appropriately to territory mobility.

The underground existing network, as shown in the Figure 1, is composed by four main lines with a total covered length of 69.25 km, which transports over 650000 passengers per day. The stations are 51 with an average distance between them of 1.5 km.



Figure 1 Existing underground network

The line 5 of Bucharest connects West to East sides of the city, in particular from Drumul-Taberei district to Pantelimon area. These two zones are served by surface transport, as buses, trolleybuses and tram and this led to high traffic congestions: a technical report on surface transport made in 2015, it showed an

average value of the commercial speed of about 13 km/h, therefore the travel time exceeded 60 minutes. Regarding the private traffic, the vehicles per day recorded are 30000 and the average velocity is 32 km/h. Hence, the need to improve the public transport network occupies a key role for the future of the city, in order to address to the phenomenon of urban congestion.

The scopes of the work are:

- Accessibility;
- Minimum time on the origin-destination route;
- Safety and comfort of the passengers;
- Minimize environmental impacts (noise, pollution, land use...);
- Improve the transport capacity;
- Modernize public transport infrastructures.

The pathway of line 5 crosses the city of Bucharest in a West to East direction joining three major areas: Drumul Taberei district, Bucharest Centre and Pantelimon district.

The line 5 Drumul Taberei - Pantelimon includes 22 stations: Valea Ialomitei, Raul Doamnei, Brancusi, Romancierilor, Parc Drumul Taberei, Drumul Taberei 34, Favorit, Orizont, Academia Militara, Eroilor, Hasdeu, Cismigiu, Universitate, Calea Mosilor, Traian, Piata Iancului, Victor Manu, National Arena, Chisinau, Morarilor, Sfantul Pantelimon, Vergului.

The line 5, Figure 2, allowed the interconnections with the others metro lines in correspondence of the stations Eroilor, Universitate and Piata Iancului.

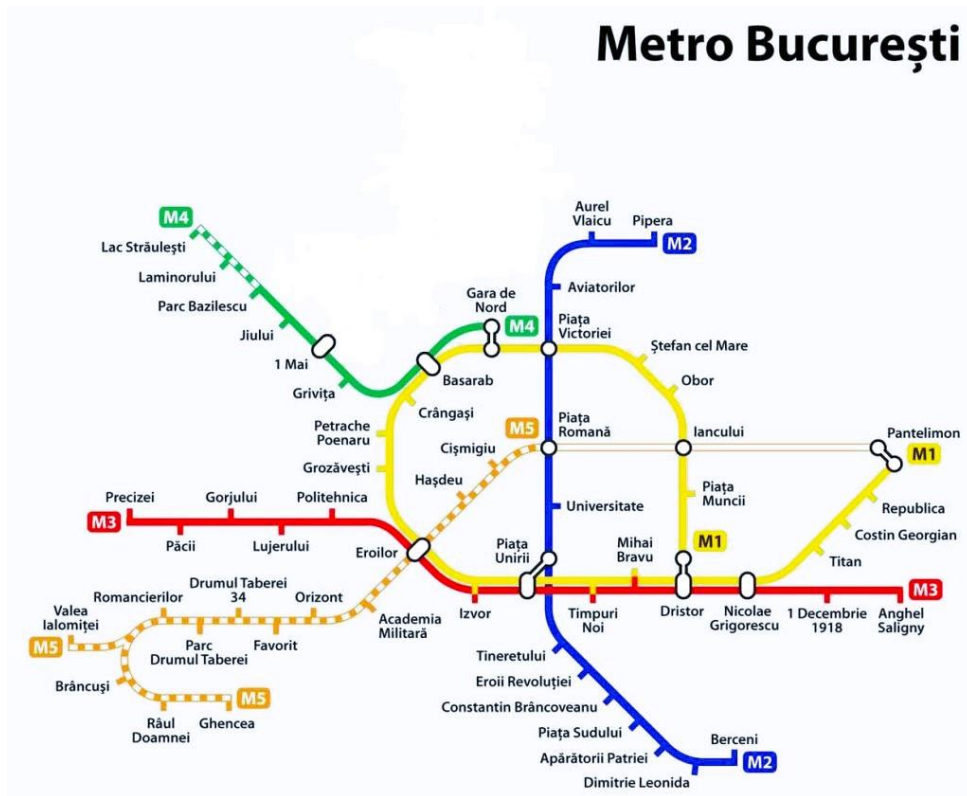


Figure 2 M5 metro line

The project is subdivided in the construction of three main structures:

- Tunnel, which is constructed with mechanised shield method or with cut and cover open excavation;
- Station: open excavation supported by temporary and permanent structures;
- Gallery: it is an extension of the station structures used for manoeuvring and is built in open excavation.

The stations and galleries are constructed by top-down procedure because of not enough space on the surface and time restriction. The overburden of the station is at least 2 meters. The selected construction method involves the execution of diaphragm walls and slabs from top to bottom in order to ensure the stability and sealing of the excavation enclosure.

The tunnel is excavated with Earth Pressure Balance EPB machine, which is able to adjust the excavation pressure based on the characteristic of the soil. The operational mode of the machine is Fully Closed mode. The general design aspects are:

- The overburden is from 10 to 14 meters, also reaching 28 meters. In order to guarantee the stability condition, a minimum overburden is considered, as 1.5 times the diameter of the machine;
- The internal diameter of the segmental lining is 5.7 meters;
- The thickness of the segmental lining varies between 25-35 centimetres;
- The width of the segmental lining ranges between 1 – 2 meters.

1.1. Geological and hydrogeological data

From the geological point of view, the Bucharest area can be classified in seven main layers, starting from surface as shown in following Figure 3 (in bracket, the thicknesses are highlighted):

1. Anthropogenic filling and top soil (3 – 10 m);
2. Upper clay sandy complex which is subdivided in three sub-complexes: Dambovita-Colentina interfluvial domain (2 – 5 m), Baneasa-Antelimon (10 – 16 m) and Cotroceni-Vacaresti (3 – 6m);
3. Colentina gravel complex (1 – 20 m);
4. Intermediate clay layer (0 – 25 m);
5. Sands of Mostistea (1-25 m);
6. Lake complex (20-50 m);
7. Fraternal complex.

From the hydrogeological point of view, the Dambovită River crosses the route of the future metro in the left side. In addition, there is the presence of three main aquifers in a depth range between 4 and 50 meters (Figure 3):

- The aquifer of Colentina gravel is made up of coarse sediments and it is located at a depth of 15-20 meters. The hydraulic conductivity is about 20 m/day.
- The sands of Moistitea aquifer is located at 20 – 42 meters depth. Its hydraulic conductivity has a value, which ranges between 3-15 m/day.
- Fratești aquifer system is a confined aquifer.

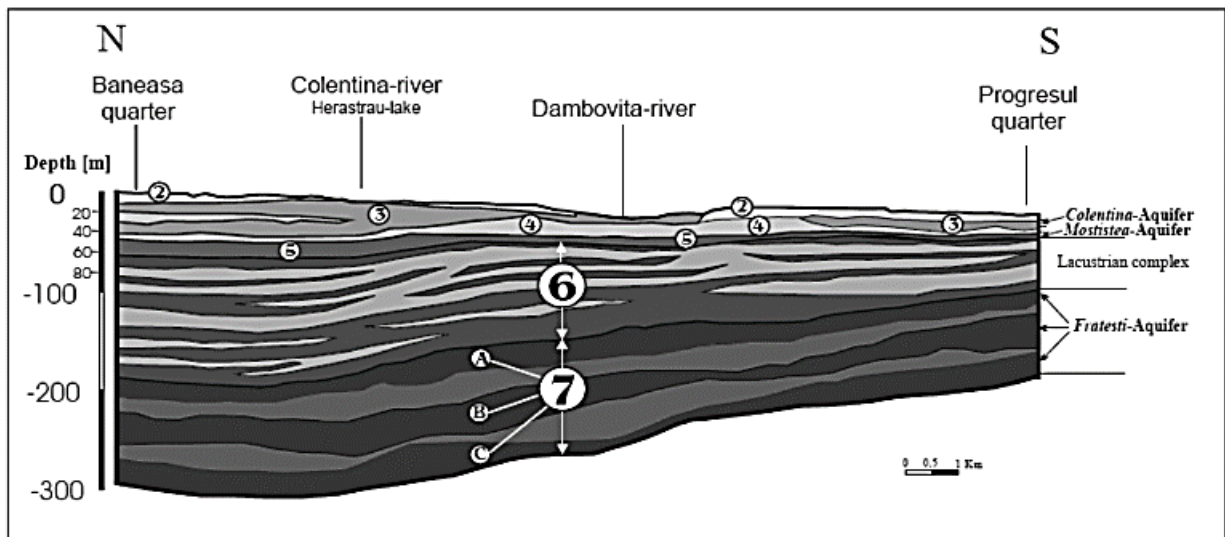


Figure 3 Stratigraphy of the project area

1.2. Earth Pressure Balance:

The Earth Pressure Balance Shield Machine, Figure 4, provides support on the face front and on the cavity. The support of the cavity is guaranteed thanks to the presence of the steel shield. On the other hand, the face stability is provided with the treated excavated soil.

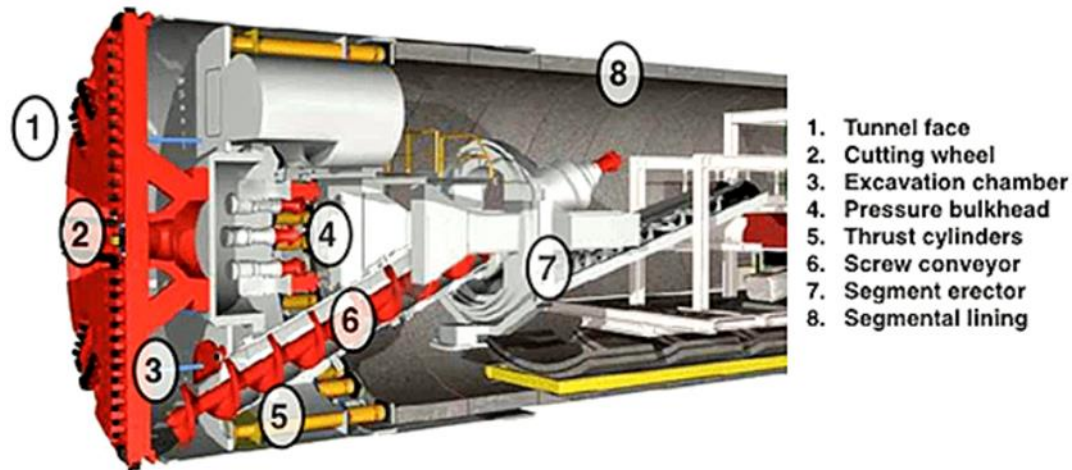


Figure 4 Earth Pressure Balance machine (EPB)

The EPB machine has different advantages with respect to slurry shield or compressed air machines: it is able to better control the surface settlement, and it does not require a separation plant for the re-use of the bentonite, leading to the reduction of the needed space on the surface and of costs.

The excavation of the soil is provided by the rotation of the cutter head, which has particular cutting tools based on the type of ground. The advancement of the machine is allowed by the thrust jacks that push against the face front. This produces an excavated material, which is suddenly treated with conditioning agents to better transfer the advancement pressure.

The excavated material, after it is modified or conditioned, comes out from the excavation chamber through a screw conveyor. It has two main goals:

- Transport the excavated material from the excavation chamber to the conveyor belt;
- Regulate the pressure inside the chamber to counterbalance the groundwater and ground pressures.

By adjusting the speed of the cochlea, the applied support pressure changes because the amount of conditioned soil inside the chamber changes. At the end

of the screw conveyor, there is the conveyor belt. An important point to make is that at the end of the cochlea, the pressure must be nil in order to better lie down on the conveyor belt. So the length and the inclination of the screw help to reduce the pressure, usually 0.2 bar per helix. Once the muck is on the conveyor belt, it arrives outside the tunnel and then is transported to the surface. The conveyor belt is able to storage and incorporate the belt by advancing in order to cover the entire length of the excavation from the screw up to the outside. It is called extendible conveyor belt and it is possible to incorporate about 400-500 meters.

The advancement is mainly guaranteed by the thrust, while the excavation by the torque transmitted at the cutter head.

The thrust force (ΣW) is applied by the hydraulic thrust cylinders, which are located all around the circumference of the machine. The thrust is transferred from these elements to the conditioned soil through the bulkhead in order to avoid uncontrolled penetration. It depends predominantly on the friction of the shield coat during the passage inside the soil, on the maximum applicable thrust force of the single tool and on the requested support pressure. A limit is the resistance of the single segment: since the cylinders are able to apply a force only by pressing against the lining, if the stress overpasses its strength, the breakage of the segments occurs. The thrust is computed as follows:

$$\Sigma W = W_M + W_{Sch} + W_{BA} + F_S + F_{NL} + F_{SP}$$

Where:

- W_M is the friction of the shield coat;
- W_{Sch} is the thrust resistance of the cutting edge;
- W_{BA} is the maximum tool thrust force;
- F_S is the drag force tailskin seal;

- F_{NL} is the drag force back-up system;
- F_{SP} is the support pressure.

However, the torque (T) is provided by several hydraulic motors, which transmit the rotation to the cutter-head via a gear rim. The torque is empirically evaluated by taking into account the diameter of the machine (D) and a coefficient (α), which has been evaluated studying a huge amount of case histories. A significant variation of this last parameter during the excavation can be an evidence of problems, which are occurring in the excavation chamber.

$$T = \alpha * D^3$$

The α coefficient has a high value compared to that one for the slurry machines because of the greater density of the conditioned material: in fact, it ranges between 2 – 3 for the EPB and 0.75 – 2 for the slurry.

The EPB machine is equipped with a system for the final lining installation. After completing a cycle of advancement, a ring of lining is installed. There are three existing types of rings:

- Rectangular ring which has all the sides equal;
- Tapered ring that has one side perpendicular and the other inclined with respect to the longitudinal direction;
- Universal ring with both the sides inclined.

Nowadays the most used is the universal one and so the difference of the two sides, called tapering (ΔL), must be evaluated with the following formulation:

$$\Delta L = \frac{R_e - L}{0.8 * R_t}$$

This formula depends on:

- R_e is the radius of the ring at the extrados;

- L is the length of the smallest side;
- R_t is the radius of the alignment.

Every ring is composed by pre-casted elements called segments divided in three families: normal, counter-key and key one. Typically, the number of the segment for each ring is six. The thickness of the lining ranges normally from 30 to 70 cm and it can vary depending on soil and water pressures.

Segments are assembled starting from the bottom element up to the key: their installation is made by an erector that works with vacuum. Since they are installed below the shield where the confining pressure is not acting, the stability is guaranteed by elements like connectors, bolts and dowels. Moreover, the water tightness is ensured by the gasket which is a rubber element glued all around the segment.

The segments are produced in a plant close to the construction site in a quantity that guarantees the continuous feeding of the machine.

The main problem with the use of a tunnel boring machine is the formation of an annular void due to the overcut of the cutter head, the conicity of the shield, the thickness of the shield and the thickness of the steel brushes as shown in the Figure 5. If this gap is not filled just after its formation, a ground surface settlement can arise. The dimension of the annular gap ranges between 10 and 20 centimetres.

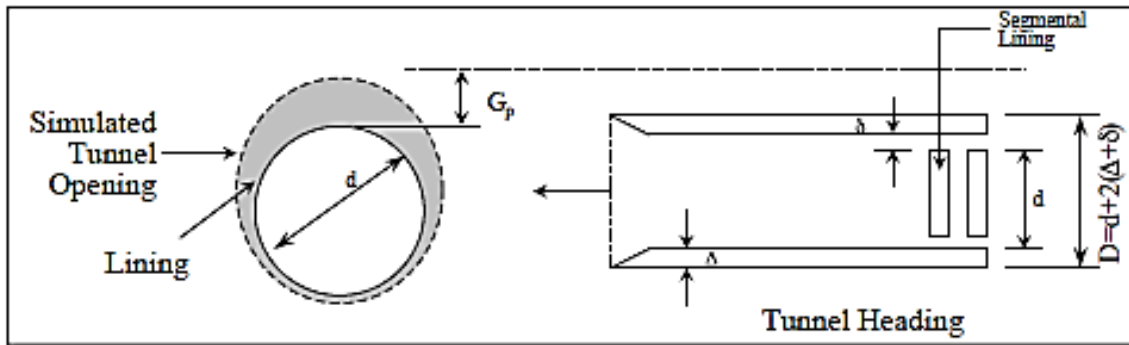


Figure 5 Dimension of the annular gap (Loganathan, et al., 1998)

The solution of this problem is the backfilling. Nowadays, the most used grout for this purpose is the two-component grout. This material is characterised by two parts: the component A and the component B. Water, cement, bentonite and retarding/fluidifying agent compose the first one, while the second one is only an accelerator. This innovative solution led to a series of advantages:

- it reduces the vertical displacement whatever the soil is;
- it is able to enter in the gap with small energy reducing the load on the coatings due to the small viscosity;
- the storage capacity is high due to the presence of the retardant;
- the mechanical performances are developed in a few seconds after the injection;
- the permeability is very low due to the presence of the bentonite;
- the resistance to the water washout is very high due to the almost immediate gelification;
- low risk of blockage of the injection pipes thanks to the absence of aggregates and the use of bentonite;
- very easy transport and pumpability because the low viscosity and great volumetric stability;
- the practicability in the use of this material in relation to the reduction of the operative action to install it.

The implementation of this grout is in continuous during the advancement with an injection from some grouting ports on the tailskin at a pressure greater than that of the excavation in order to minimise the immediate displacements.

The Earth Pressure Balance machines nowadays are the most used machines in the world for the projects in shallow tunnel in urban area. When the soil has stiff consistency ($I_c > 1$), high cohesion and low permeability it is possible to work without support pressure.

If a support pressure is needed, it is applied mainly thanks to the excavated material. However, it is difficult to obtain a uniform pressure distribution only with soil. Hence, it is necessary to condition the material. This procedure can be done using different substances based on the grain size distribution of the soil and the percentage of passing through the sieves, as shown the Figure 6 (DAUB, 2016). The conditioning can be obtained only with water for soils falling in Area 1. If the material is coarser and it falls in Area 2, foam is added. When the soil becomes coarser and more grained like in Area 3, the soil is conditioned with foam, water and, if necessary, with bentonite, filler and different types of additives like polymers and anti-clogging. The permeability and the groundwater pressure determine the limits of application: in fact, the permeability should not exceed the 10^{-5} m/s.

Moreover, the diameter of the chips should be limited since EPB machines not provided of a crusher: the consequence could be the damage of the screw conveyor.

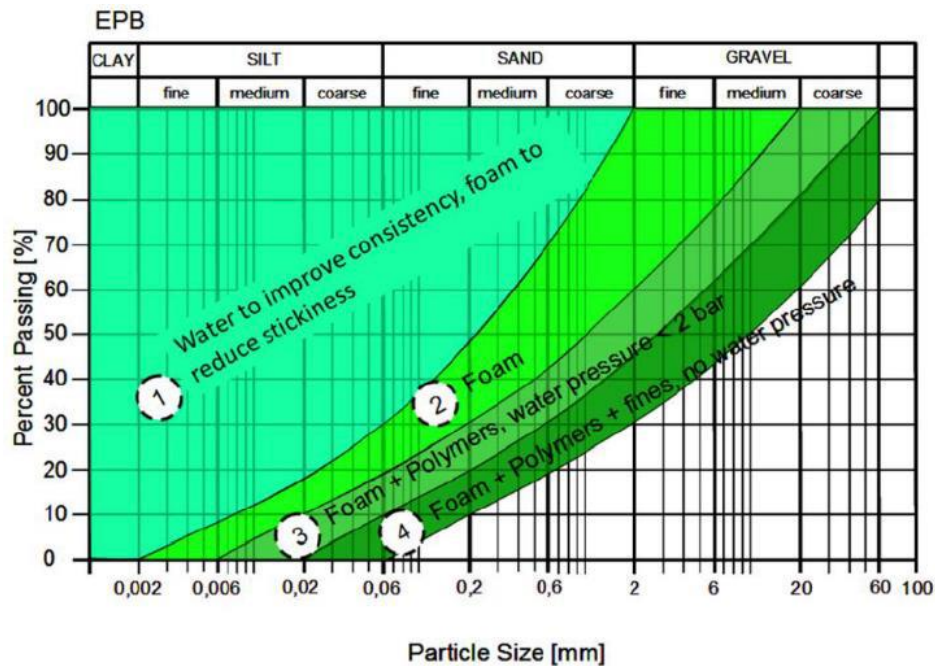


Figure 6 Selection of the conditioning agent based on the grain size distribution (DAUB, 2016)

The cutterhead of the machine has large percentage of aperture: higher is the opening, lower is the amount of cutting tools. The selection of the cutting tools is based on the type of encountered soil, the resistance and the abrasiveness of it, the content of clay or quartz. On the periphery of the circular head, there are also the overcutting tools, which permit an over-excavation in order to help the shield to pass easily and to not block inside the above and bottom soil. Always on the face there are different nozzles to spray the conditioning agents, so this allows to mix the soil ahead of the face and then to enter in the chamber.

To support and provide the rotary movement to the cutting head, there is the main drive. It is composed by several hydraulic motors, which works in parallel in order to transfer the motion to the head. This part is always filled with grease because it avoids the entrance of particles inside the gear, which can be seriously damaged.

On the upper part of the EPB, the air lock is fundamental when it is necessary to enter in the working chamber by the personnel. This part allows the

acclimatization to the pressure in the chamber, in entrance, or to the atmospheric pressure at the return. The presence of the air lock is fundamental for avoiding health problems during the permanence of the personnel, because inside it they are exposed to a gradually increase of pressure.

2. SETTLEMENT INDUCED BY SINGLE AND TWIN TUNNELS

The excavation in the ground subsurface inevitably led to settlements.

The TBM tunnelling produces a ground movement towards the excavation centre line. This phenomenon is triggered by a ground loss that is caused by the stress relaxation because of the creation of the void. The settlement can depend on both the tunnelling process itself and the boundary conditions of the nearby of the excavation zone.

It is possible to distinguish four contributions, which compose the overall ground settlement caused by the TBM excavation procedure (Figure 7):

- Settlement above and ahead the excavation face (face loss);
- Settlement along the shield (shield loss);
- Settlement in correspondence of the tail skin (tail loss);
- Settlement related to the shrinkage of the grout at long term.

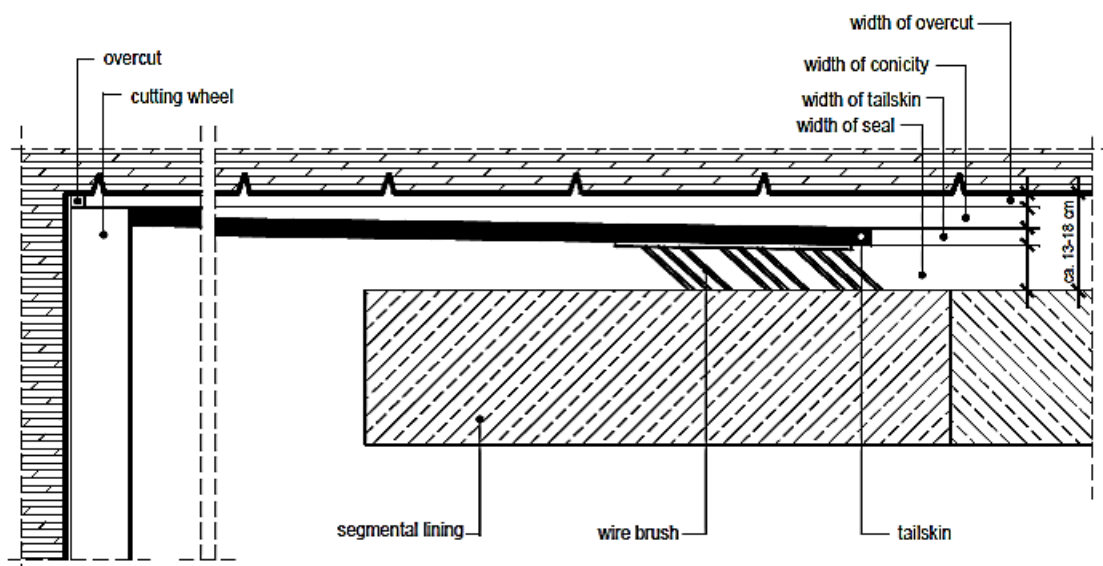


Figure 7 Contribution of the overall ground settlement

The **face loss** occurs due to the decompression of the tunnel face depending on the difference in pressure between the one applied by the machine to stabilize

the front and the geostatic stress. For this reason, during the advancement, the soil surrounding the face, above and ahead, moves towards it. It is possible to estimate in percentage this value by the following formulas (Lee, et al., 1992):

$$V_f = \frac{g_f}{R} * 100\%$$

$$g_f = \frac{k * \Omega * R * P_0}{2 * E}$$

$$P_0 = k_0 * P_v + P_w - P_i$$

Where:

- g_f is the equivalent gap at the crown of the face loss;
- R is the tunnel radius;
- k represent the resistance between the intruding soil and the TBM chamber skin;
- Ω is the dimensionless axial displacement ahead of the tunnel face;
- P_0 is the total stress removal at the tunnel face due to the excavation;
- E is the elastic modulus at the tunnel spring line;
- k_0 is the earth pressure coefficient at rest;
- P_v is the effective ground pressure at the spring line;
- P_w is the water pressure;
- P_i is the TBM face pressure.

The **shield loss** takes place because of the radial movement of the ground. This component is induced by the designed overcutting of the rotating wheel, the guidance issue of the shield (its tendency to pitch and yaw can produce an increase of the size of the created radial void) and the conicity of the shield. This contribution is computed thanks to the equation below:

$$V_s = \frac{g_s}{R} * 100\%$$

$$U_i = R(1 + \nu) * \frac{(\gamma * H + P_w - P_i)}{E}$$

$$g_s = \begin{cases} \text{if } U_i > t_t + t_b \rightarrow g_s = 0.5 * (t_t + t_b) \\ \text{if } U_i \leq t_t + t_b \rightarrow g_s = 0.5 * U_i \end{cases}$$

Where:

- g_s is the equivalent gap at the shield;
- U_i is the ground movement into the shield gap;
- ν is the Poisson's ratio;
- γ is the unit weight of the soil;
- t_t is the portion of the shield gap related to the taper;
- t_b is the portion of the shield gap related to the overcut.

The amount of the **tail loss** is composed by two contributions: the thickness of the tail skin (t) and the clearance for the erection of the segmental lining (δ). The main reason of the last input is the presence of the steel brushes. These devices, coupled with grease, are able to seal completely the inner part of the machine from the grout and groundwater. However, the entity of this gap, that could result in ground settlements, depends on the backfilling technique, on the correctness of installation and on the ability to completely fill the gap.

The backfilling grout, at long term, can undergo to **shrinkage** phenomenon, expressed as a volume loss due to the loss of water, especially in dry environment. The ground loss component due to the shrinkage of the grout is calculated as shown:

$$V_{shr} = \frac{g_{shr}}{R} * 100\%$$

$$g_{shr} = 0.1 * (t + \delta)$$

Moreover, another source of settlement is related to the groundwater. In particular, it is possible to subdivide this contribution in two classes based on the condition in which the project falls:

- The first class regards the lowering of the water table before the beginning of the excavation: this drawdown induces a sudden displacement especially in the compressible layers.
- The second class is about the changes in volume at the end of the consolidation process in cohesive saturated soils. Due to the excavation, an excess pore pressure develops and, at short term, because of the low permeability of the soil, any change in volume occurs. During the consolidation process a change in volume arises because of the dissipation of the excess pore water pressure.

Finally, the induced vibration must be taken into account as cause of displacement. Obviously, this aspect has to be coupled with the type of soil about the propagation of the seismic waves.

Once the overall volume loss at the tunnel level is determined, its propagation at the surface needs to be evaluated. The simplest mechanism of transmission of this displacement is to assume the soil as incompressible and so the recorded settlement at surface is equal to the volume loss at the opening section. In good approximation, this assumption is valid only for shallow overburden made of cohesive soils.

In reality, the surface settlement is lower, in particular by considering the following conditions:

- A wide cover produces up to 80% of the deformation damping;

- The presence of a stiffer layer over the tunnel reduces the transmission of the displacement by bridging effect;
- The existence of dilating material layer in the overburden decreases the settlement because of its tendency to deform.

However, each case is different by the others and so it not possible to define a law, which put in relation the volume of the surface settlement and the volume loss at the tunnel. In addition, the required time employed by the displacement to reach the surface must be studied case by case

2.1. Shape of the zone of influence

After these considerations, the next step is the identification of the shape of the settlement trough and the size of the zone of geotechnical influence.

The first author, who has examined this aspect, is Martos (1958). He stated that the trough could be represented by a Gaussian curve. Other authors, Schmidt (1969) and Peck (1969) after some years, confirm this conclusion.

The settlement curve, Figure 8 is characterised by two zones: the sagging and the hogging areas. The first one is the concave zone, while the other is the convex one. The separation of the two zones is the so-called inflection point. In addition, it is possible to define other two points: the maximum curvature of sagging and the maximum curvature of hogging.

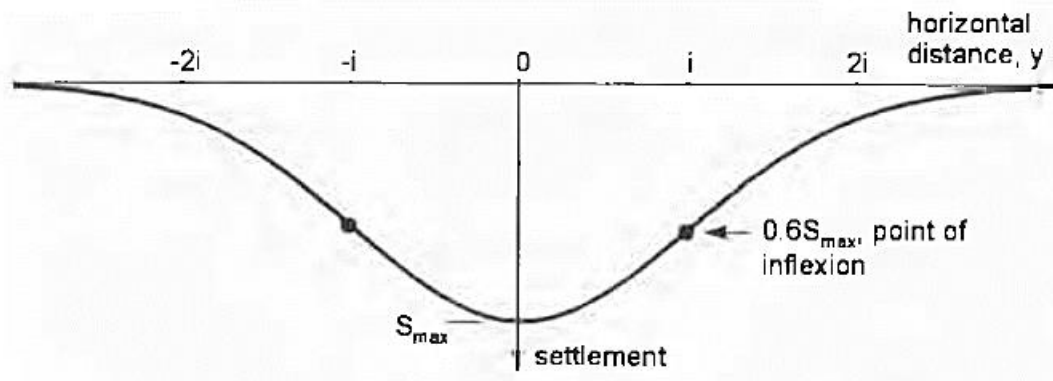


Figure 8 Shape of the settlement trough (Mair, et al., 1997)

The influence zone, and so the width of the subsidence trough, is considered, empirically, ranging from 2.5 to 3 times the horizontal distance between the centre line and the position of the inflection point. This limit value does not always represent the point in which the displacements are equal to zero, but it is a threshold after which the settlement no longer creates problems to the pre-existing buildings.

2.2. Evaluation of the surface settlement

The possible ways in which it is possible to compute the settlement induced by the tunnelling excavation can be classified in three categories:

- Empirical methods;
- Semi-empirical methods;
- Analytical methods;
- Numerical methods.

In this chapter, a global overview of these methods will be presented highlighting their main aspects.

2.2.1. Empirical method

This is the simplest method that allows the calculation of the surface settlement. It takes into account several features as the dimension of the excavation, the height of the overburden, the ground condition and the induced volume loss.

The method is based on a pseudo-elastic analysis and it gives as output the maximum surface settlement.

$$S_{MAX} = K * \lambda * \frac{\gamma * R^2}{E}$$

Where:

- K is an empirical constant related to the condition of the ground;
- λ is the stress release coefficient;
- γ is the average unit weight of the ground;
- R is the radius of the tunnel;
- E is the Young's modulus of the ground.

This empirical formula allows an easy evaluation of all the unknowns for the calculation of the surface settlement through a parametric analysis and, in the common practice, it is coupled with the analytical or numerical methods in order to calibrate them.

Nevertheless, it is considered a very simplistic approach because it does not take into account the tunnel depth and it is not applicable for shallow tunnels due to the non-uniformity of the stress field when the depth is lower than three diameters.

For these reason, the empirical method is widely used nowadays to perform the preliminary study stage.

2.2.2. Semi-empirical method

The most popular semi-empirical method is the one proposed by Peck (1969). It represents the transversal settlement trough (S_v) like a Gaussian distribution considering a green field condition at coordinate $y=0$. For the width of the subsidence trough (i) O'Reilly, et al. (1982) provide a formula below.

$$S_v = S_{max} * \exp\left(-\frac{x^2}{2i^2}\right) = \frac{V_L}{i\sqrt{2\pi}} \exp\left(-\frac{x^2}{2i^2}\right)$$

$$i = Kz_0$$

Where:

- S_{max} is the maximum settlement at the surface centre line;
- x is the lateral distance from the tunnel centre line;
- i is the horizontal distance between centre line and the inflection point;
- K is the trough width parameter (it ranges from 0.4 to 0.7 for cohesive soils and from 0.2 to 0.3 for granular soils);
- V_L is the volume loss that is commonly lower than 0.5% (it expresses the ratio between the ground loss volume and the tunnel volume per meter length);
- z_0 is the depth of the tunnel from the tunnel axis.

The longitudinal settlement in green field condition, instead, is evaluated thanks to the equation derived by Attewell, et al. (1982). The main assumption is that the subsidence trough increases in size during the advancement following a cumulative frequency function.

$$S_x = S_{max} \left[G\left(\frac{x - x_i}{i_y}\right) - G\left(\frac{x - x_f}{i_y}\right) \right]$$

Where:

- G is the cumulative distribution function;
- x_i is the initial position of the tunnel face;
- x_f is the final position of the tunnel face.

The trough width parameter in longitudinal direction is taken equal to the transversal one for practical estimation purposes.

By combining the equations for the transversal and longitudinal settlement, the following equation by Attewell, et al. (1982) allows to evaluate the three-dimensional induced settlement:

$$S_{x,y} = S_{max} * \exp\left(-\frac{x^2}{2i(z)^2}\right) * \left[G\left(\frac{x - x_i}{i_y(z)}\right) - G\left(\frac{x - x_f}{i_y(z)}\right)\right]$$

2.2.3. Analytical method

An analytical method is based on the resolution of equations and on hypothesis to simplify the reality:

One of the few analytical solution is the closed-form solution by Loganathan, et al. (1998) which derives from the Verruijt, et al. (1996) formulation. The latter one estimates the settlement and the deformation considering different values of the compressibility of the soil, including the ovalisation of the lining. The innovations provided by the Loganathan and Poulos are:

- a. Introducing realistic ground loss boundary conditions;
- b. Considering an oval shape of the annular void generated by the effect of the gravity.

They assess that the 75% of the vertical displacement come from the upper part of the annulus. The zone in which the displacements occur is characterised by a limit angle β from the horizontal and the magnitude of the horizontal movement

at the spring line is equal to the half of the vertical displacement of the crown of the tunnel. The closed-form solution is reported below:

$$U_{z=0} = \varepsilon_0 * R^2 * \frac{4H(1 - \nu)}{H^2 + x^2} * \exp \left[- \frac{1.38x^2}{(H * \cot\beta + R)^2} \right]$$

$$\beta = 45^\circ + \frac{\phi}{2}$$

$$k_0 = \frac{\nu}{1 - \nu}$$

Where:

- $U_{z=0}$ is the ground surface settlement;
- R is the tunnel radius;
- H is the depth of the tunnel axis level
- k_0 is the earth pressure coefficient at rest;
- ν is the Poisson's ratio of the soil that is computed from the formula of the k_0 ;
- ε_0 is the average ground loss ratio;
- x is the lateral distance from the tunnel centre line;
- β is the limit angle;
- ϕ is the friction angle of the soil.

The width of the settlement trough (i), useful to compute the zone of influence of the tunnel, can be computed by the proposed formula:

$$\frac{i}{R} = \frac{1.15}{(\tan\beta)^{0.35}} * \left(\frac{H}{2R} \right)^{\frac{0.9}{(\tan\beta)^{0.23}}}$$

This equation provides a correlation between the normalised trough width and the normalised depth.

2.2.4. Numerical method

The numerical methods are nowadays more popular than the empirical and analytical one because allow to simulate a detailed construction process, to include the ground behaviour through defined constitutive laws, to take into account complex hydraulic conditions and treatments to which the ground undergoes.

The use of the Finite Element Model (FEM) requires high competence, modelling and interpretation skills to obtain accurate results. They allows to simulate:

- The real stress path that the ground (soil-structure interaction mechanism) undergoes during the tunnel excavation changing the excavation method;
- The three-dimensional effect of different volume losses (face loss and radial loss);
- The stress-strain behaviour in the surrounding zone of the tunnel.

Even if one of the main characteristic of the tunnelling process is the three-dimensional nature, the numerical analysis are usually done in two-dimension in the transversal direction respect to the advancement, by assuming plain strain condition. The two-dimensional analysis are faster and requires less computational efforts.

However, some limits exist as the complexity in its implementation and the tendency to overestimate the zone of influence for shallow depth tunnel. Hence, a validation of the model must be done in order to correctly calibrate it.

The 2D FEM analysis is based on eight steps:

1. Domain definition: identification of the boundaries of the model with a sufficient distance from the analysed zone in order to do not influence the results;
2. Discretization of the model: subdivision of the domain in small subdomains, which constitute the so-called mesh;
3. Definition of the primary variable: the displacement is computed by a polynomial expression of order equal to the number of the node of the element and it is valid only within itself.
4. Single element equations: the polynomial expression can be written in form of a vector through a product of the matrix $[\phi]$ and the vector of the generalised coordinates $\{\alpha\}$.

$$\{u\} = [\phi]^T \{\alpha\}$$

It possible to compute the displacement on the nodes of the element multiplying the matrix of the coordinates of the nodes and the vector $\{\alpha\}$.

$$\{u\}_e = [A]\{\alpha\}$$

Now, the initial equation can be re-written finding the shape function matrix $[H]$.

$$\{u\} = [\phi]^T [A]^{-1} \{u\}_e = [H]^T \{u\}_e$$

The deformation equation can be computed deriving the displacement one. Hence, the strain equation depends on the element strain matrix $[B]$ and the vector of the nodal displacement $\{u\}_e$.

$$\{\varepsilon\} = [B]\{u\}_e$$

The stresses are retrieved by assuming the linear elastic model and depends on the strain and the elasticity matrix $[C]$.

$$\{\sigma\} = [C]\{\varepsilon\}$$

At this point, the relationship between the nodal forces $\{X\}_e$ and the nodal displacements $\{u\}_e$ are introduced thanks to the stiffness matrix $[K]_e$.

$$\{X\}_e = [K]_e \{u\}_e$$

5. Global equations: the single element equations can be assembled in order to set a global equation extended to the entire mesh by using a global stiffness matrix.

$$\{X\} = [K]_G \{u\}$$

6. Application of the boundary conditions: there are two families of them, in particular, the load conditions (punctual or distributed) and the boundary displacement condition of the domain (imposed through hinges or rollers).
7. Solution of the global equations: the outputs are the displacements, the stress and strain on each node.
8. Interpretation of the results: this last step has a crucial importance because it allows the validation of the results by the comparison the monitoring data.

The three-dimensional FEM analysis allows to obtain the main feature of the tunnelling process linked to the advancement process of the face front and to study complex construction schemes.

In order to build a 3D FEM model seven steps must be followed:

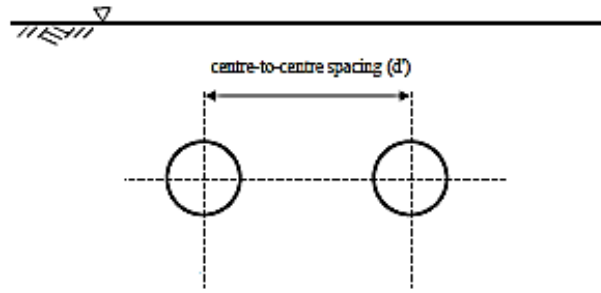
1. Discretization of the problem creating the finite element mesh;
2. Definition of the boundary conditions: they are fixed in term of displacements by applying rollers and hinges at the boundaries;
3. Assignment of material properties to the elements;

4. Initial stress state definition: there are two ways of assigning it: to perform a stress analysis by applying gravity loading or to assign directly in-situ stresses in each node;
5. Computational stage to simulate the construction sequence;
6. Computation;
7. Interpretation to analyse and validate the results.

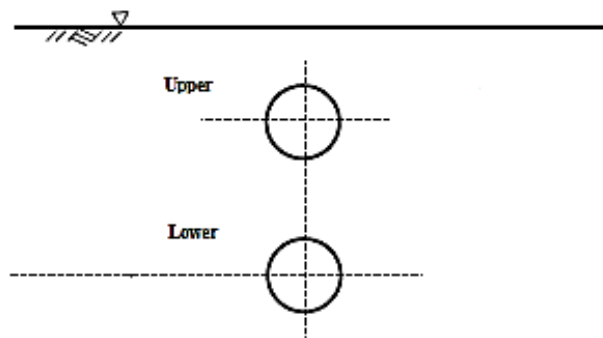
2.3. Twin tunnels

Nowadays, because of the rapid expansion of the cities, a sudden increase of the construction in underground is registered especially for the subway-transportation system. Consequently, the design of closed-spaced tunnels becomes a standard owing to a lack of underground space. There are three main layouts used to the disposition of the twin tunnel in the underground, as shown in the Figure 9:

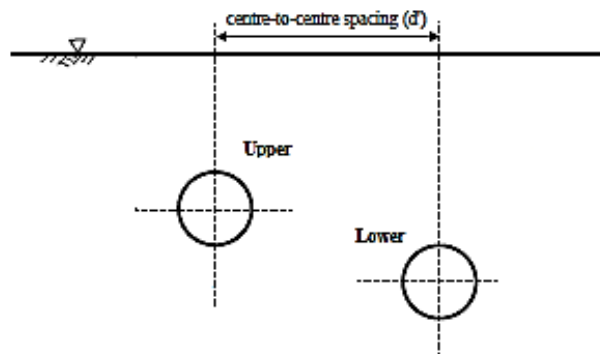
- Side-by-side tunnels;
- Piggyback tunnels;
- Offset tunnels.



(a) Twin side by side tunnel geometry



(b) Twin piggy back tunnel geometry



(c) Twin offset tunnel geometry

Figure 9 Twin tunnels layouts (Hunt, 2005)

The ground-surface settlement prediction is obtained by the superimposition of the single subsidence troughs.

Exclusively, for the side-by-side configuration it is possible to identify a semi-empirical formula proposed by (New, et al., 1991):

$$S_v = S_{max} * \left\{ \exp \left[-\frac{x^2}{2i^2} \right] \right\} + \left\{ \exp \left[-\frac{(x-d)^2}{2i^2} \right] \right\}$$

where d is the spacing of the two tunnels and the other parameters are already explained before.

The problem with the using of this equation is that it does not take into account the fact that the twin tunnels do not are built simultaneously, but with a certain delay between them. It can cause, in the subsidence trough of the tunnel excavated as second, an asymmetry of the settlement distribution, an eccentricity of the maximum vertical displacement and an increase of the volume loss.

For a more realistic computation of the subsidence induced by twin side-by-side tunnels, Hunt (2005) has postulated a modification factor M , able to fulfil to the abovementioned deficiencies, except for the volume loss issue. The new formulation related only to the second tunnel is:

$$S_{v,mod} = \left\{ 1 + \left[M * \left(1 - \frac{|d + x|}{AK_1z_0} \right) \right] \right\} S_{max} * \left\{ \exp \left[-\frac{x^2}{2(K_2z_0)^2} \right] \right\}$$

where A is the coefficient, which is multiplied for the trough width in order to obtain the full size of it, normally ranges from 2.5 to 3. After the analysis of several cases, Hunt recommends a value of 0.6 for the modification factor.

Conversely, for the other two types of layouts, empirical or analytical formulas for the surface settlement computation do not exist yet and so the only way is a numerical method analysis.

Naturally, the first tunnel affects the second one in every different layout proposed. The main parameters, which must take into account, are the spacing between them, the effect of the pre-failure soil stiffness, the change in volume loss, the changes in the settlement trough and the size of the excavation. In particular, the pre-failure soil stiffness is the condition of the soil subjected to

induced deformation by the passage of the first tunnel. After this passage, the stress-strain condition of the soil could reach the yielding point and so with the application of another load (the second tunnel) the stiffness is lower, hence the deformation is greater.

Hunt performed an analysis for each twin tunnel arrangement with the aim to investigate how the change of these parameters affects the shape of the trough and the position and magnitude of the maximum settlement.

In relation to the side-by-side tunnel, it is possible to state that the settlement related to the second tunnel is greater than that of the single tunnel. In particular, it increases of 60% for a spacing of 20 m and this increment is registered for the limb of the trough closer to the first tunnel, especially just over the first tunnel. In fact, the trough results asymmetric and can be subdivided in the near limb (limb close to the first tunnel) and remote limb (Figure 10).

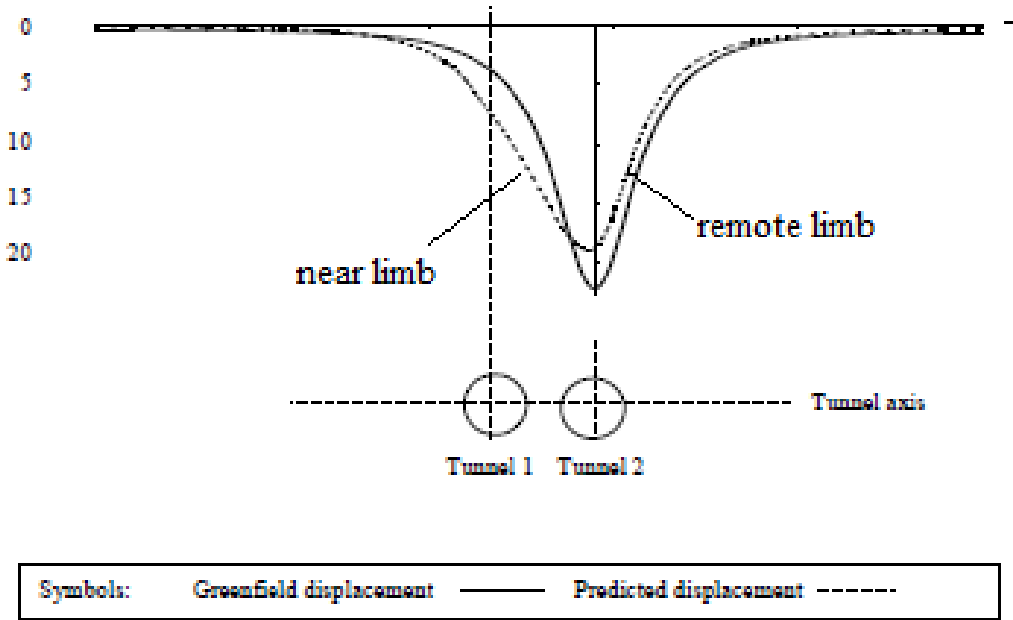


Figure 10 Limbs of the settlement trough (Hunt, 2005)

This behaviour is independent from the size of the excavation and the volume loss and it is caused by the change of the soil stiffness due to the passage of the

first tunnel. In addition, the amount of eccentricity of the maximum displacement is inversely proportional to the spacing, while decreases going deeper.

The piggyback tunnels record a different behaviour. The analysis is conducted for both the possible design choices: the upper tunnel first and the bottom first. For both the scenarios, the settlement trough of the second tunnel is symmetric and if the volume loss remains constant, any increase of the displacement is registered over the first tunnel. Regarding the outer part of the curve of the second tunnel a rise with respect to the single construction can be pointed out. Anyway, some difference can be highlighted:

- In the case of the upper constructed first, the settlement related to the second tunnel is lower compared to the single excavation: the stiffness of the lining of the above tunnel in fact improves the quality of the soil; hence, a reduction of the displacement occurs.
- On the other hand, for bottom first, the maximum displacement of the second tunnel is lower compared to the single one. This is much more evident increasing the excavation diameter because with large value of it, a heave of the soil happens. The heaving phenomenon is caused by the large amount of soil, which has been removed generating a relief of the overburden stress.

It is appropriate to specify that this behaviour is not a rule because several studies have proved that this displacement can reach the double of the single configuration due to the heavily damaged zone through which the second tunnel is built.

Finally, the offset arrangement is analysed following the same scheme of the piggyback tunnels.

The upper tunnel excavated first represents the first situation. In this case, there is a reduction of settlement generated by the second tunnel just over the first one, but the maximum displacement increases with respect to the single arrangement and its eccentricity is very low. This attitude has the same explanation of the piggyback tunnels: the stiffness of the lining helps the soil to counteract the displacements. By expanding the distance between them, the S_{\max} decreases progressively, while the eccentricity remains at small values.

If the bottom tunnel is driven first, the behaviour is a middle way between the abovementioned configurations. In fact, as the piggyback tunnels, a lowering of the maximum settlement is highlighted with respect to the single tunnel. Otherwise, the larger settlement over the lower tunnel, the eccentricity of the S_{\max} and the asymmetry of the trough are similar to the side-by-side layout, but occurs in a different magnitude.

3. BUILDING INDUCED DAMAGE

In general, the tunnelling process induces settlement in the subsurface that propagates in a certain magnitude at the surface level. These displacements could induce damage to the structures placed in the geotechnical influence zone generated by the tunnel.

Obviously, the stiffness of the building affects its response to the displacements, however, in this analysis it is not considered in favour of safety: the building and the settlement trough deform in the same way.

The analysis, nowadays, can be focused on two types of structures: the reinforced concrete and the masonry buildings. The first category tends to follow the ground deformations, being less stiff and placed on isolated foundation like the footings. The masonry structure, instead, is stiffer; hence, the distortions are reduced, in particular when its foundation is continuous as mat or grid of beam types.

The damage control parameters that led to a damage for a building are the followings, as shown in the Figure 11 (Guglielmetti, et al., 2007):

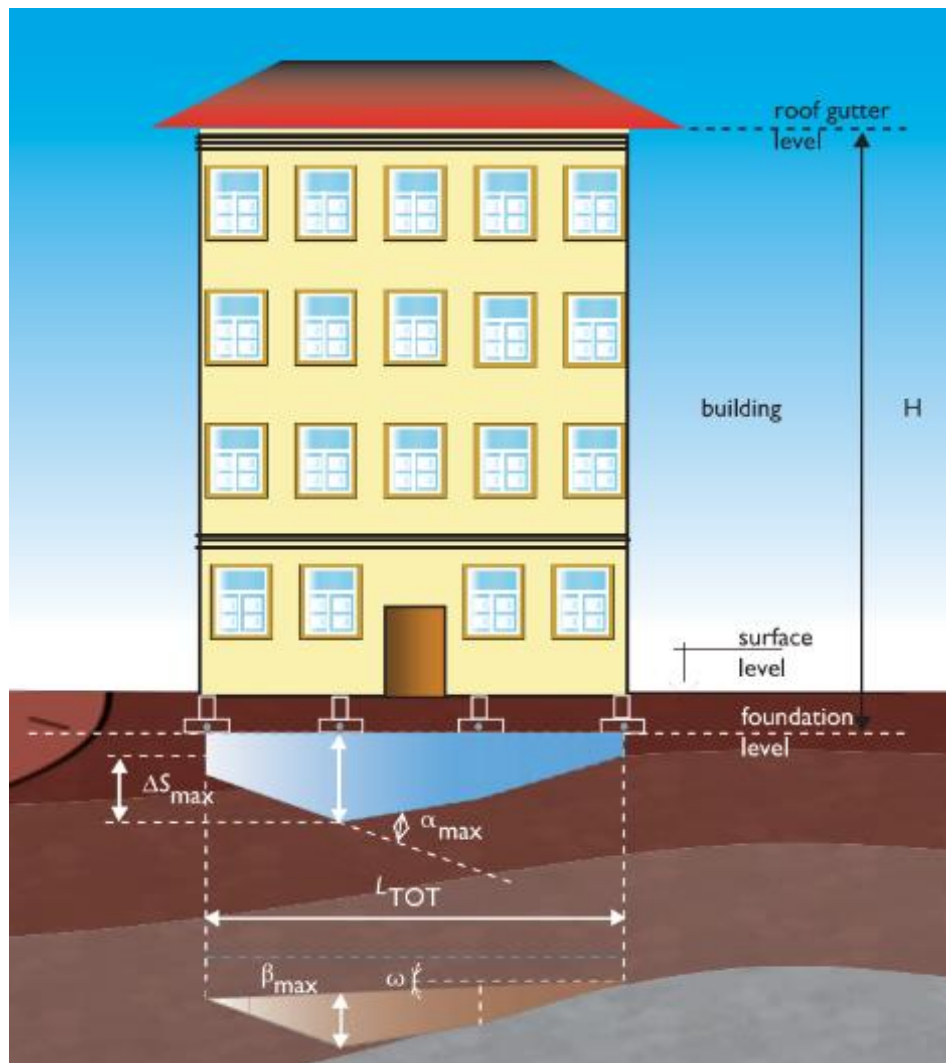


Figure 11 Damage control parameters (Guglielmetti, et al., 2007)

- S_{\max} is the maximum vertical settlement: the vertical displacement that a point express after the passage of the excavation;
- ΔS_{\max} is the maximum differential or relative settlement: the difference between the settlements of two reference point;
- α_{\max} is the maximum angular strain (positive for sagging, negative for hogging);
- ω is the tilt defined as a rigid rotation of the entire structure;
- β_{\max} is the maximum angular distortion: in a first attempt, Skempton, et al. (1956) it is defined as the ratio between the differential settlements and the horizontal distance (L) between two analysed point;

- Δ_{\max} is the maximum relative deflection: it represents the maximum vertical differential distance between the deformed foundation line and the straight connection line of the two considered points;
- Δ_{\max}/L is maximum deflection ratio obtained by dividing the maximum relative deflection by the span length (L).

The other parameter that affects the induced damage is the position of the building respect to the settlement trough. In fact, if it is placed in the hogging zone, the damage is caused by traction, while if it is on the sagging zone the structure undergoes to compression.

The damage risk assessment of the buildings induced by the ground surface settlement caused by the tunnel excavation is based on two analysis campaign:

1. The Building Condition Survey (BCS) with which the real condition of the structure are detected before, during and after the excavation;
2. Building Risk Assessment (BRA) in order to estimate the potential damages related to the expected surface settlement and the vulnerability of the structure.

3.1. Building Condition Survey (BCS)

The identification of the building condition is fulfilled by the building condition survey (BCS), which must be evaluated in three-time steps: prior, during and post construction. It is characterised by the retrieving of the information about the history of the buildings, which are placed in the geotechnical influence zone of the excavation. To every structure, a unique reference number is assigned, useful to the control and the communication of the information related to each building.

The survey is based on two aspects:

- Archival research to gather information on: the age of the building, the design drawings, the type and depth of the foundations, the number of floors, the type of supporting structure, the history of previous repair work and the addition of extra floors. Research will also determine whether the building is inscribed in lists of historical or architectural assets that will make it a particularly sensitive building;
- Visual inspection of the condition of the building: all visible parts of a building will be inspected by collecting information on: usage, crack observation, verticality, list of defects and photographic records.

The output is the Vulnerability Index (I_v) proposed by Chiriotti, et al. (2000) which expresses the vulnerability of examined building. The vulnerability index ranges from 1 to 100 (Table 1) and it can fall in five families as shown in the table below where negligible stands for a building in good condition that will undergo to any damage or extremely low value of it.

Table 1 Vulnerability index

Vulnerability index I_v	Type of vulnerability
0 - 20	Negligible
20 - 40	Low
40 - 60	Slight
60 - 80	Moderate
80 - 100	High

3.2. Building Risk Assessment (BRA)

In order to classify the entity of the induced damage of a structure in a damage category, it is necessary the building risk assessment (BRA). The different types of damage that could affect a building are so divided:

1. The **aesthetic damage** is related to little cracking of the internal wall and finishes, which are easy repairable.
2. The **functional damage** represents the decreasing in functionality of at least a part of the structure, but without affecting its integrity.
3. The **structural damage** corresponds to the heave cracking and deformation that lead to partial or total collapse of the building.

For the masonry buildings or continuous foundations, Burland, et al. (1974) define a building risk assessment methodology based on the Limiting Tensile Strain Method (LTSM). They calculate the limit strain value (ϵ_{lim}) thanks to a deep beam analogy (Figure 12), which consider an elastic, isotropic and simply supported beam as representative of real structure.

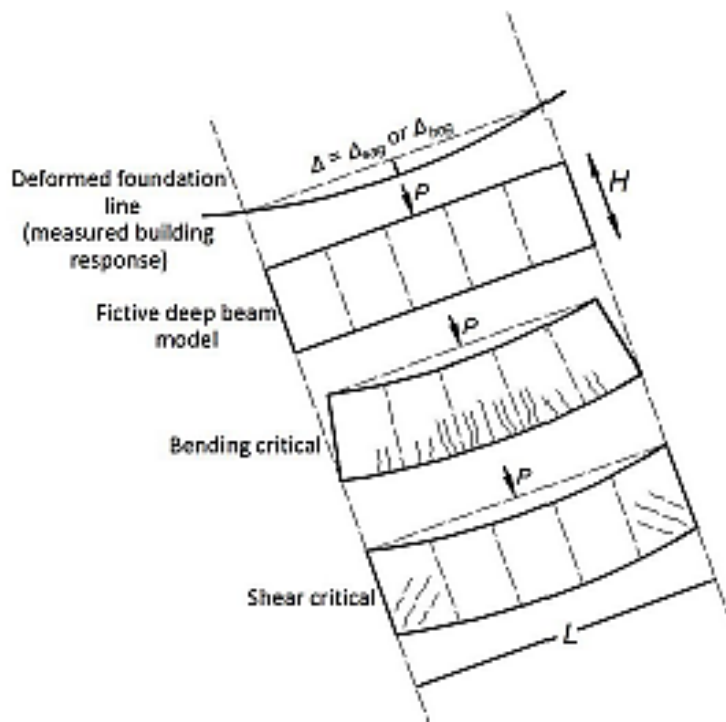


Figure 12 Deep beam model (Burland, et al., 1974)

This analysis is based on the deflection ratio index (Δ_{max}/L), which is connected with the maximum tensile strain ϵ_{max} , namely the maximum between bending

tensile strain (ε_{b_max}) and diagonal tensile strain (ε_{d_max}). These two quantities are related by the following equations:

$$\frac{\Delta}{L} = \left(\frac{L}{12t} + \frac{3EI}{2TLHG} \right) * \varepsilon_{b_max}$$

$$\frac{\Delta}{L} = \left(1 + \frac{HL^2G}{18EI} \right) * \varepsilon_{d_max}$$

Once the maximum strain is obtained, it must be compared with predefined limiting tensile strain boundaries proposed by Burland, et al. (1977).

An improvement of the aforementioned method is provided by Boscardin, et al. (1989). They include the contribution of the horizontal strain (ε_h) to the bending and diagonal tensile one, reporting that this new component can decrease the resistance of the building to the settlement coupled with the others. The horizontal strain ε_h can be calculated by the ratio between the differential horizontal displacement between two control point and the initial distance between them, as expressed in the equation below.

$$\Delta S_h = S_{h,A} - S_{h,B} = \frac{x_A}{Z_0} * S_{v,A} - \frac{x_B}{Z_0} * S_{v,B}$$

$$\varepsilon_h = \frac{\Delta S_h}{L}$$

The sign of the horizontal displacement depends on the relative position of the building with respect to the inflection points of the settlements trough. The Figure 13 below highlights all the possible conditions. Particularly, in the hogging zone the deformations induced by the vertical displacements (extension) are added to that caused by the horizontal displacements (extension). On the contrary, in the sagging zone the deformations produced by the horizontal displacements (compression) are subtracted by the one due to the vertical

displacement (extension). This behaviour leads to not consider the deformations induced by the horizontal displacements in the sagging zone in favour of safety.

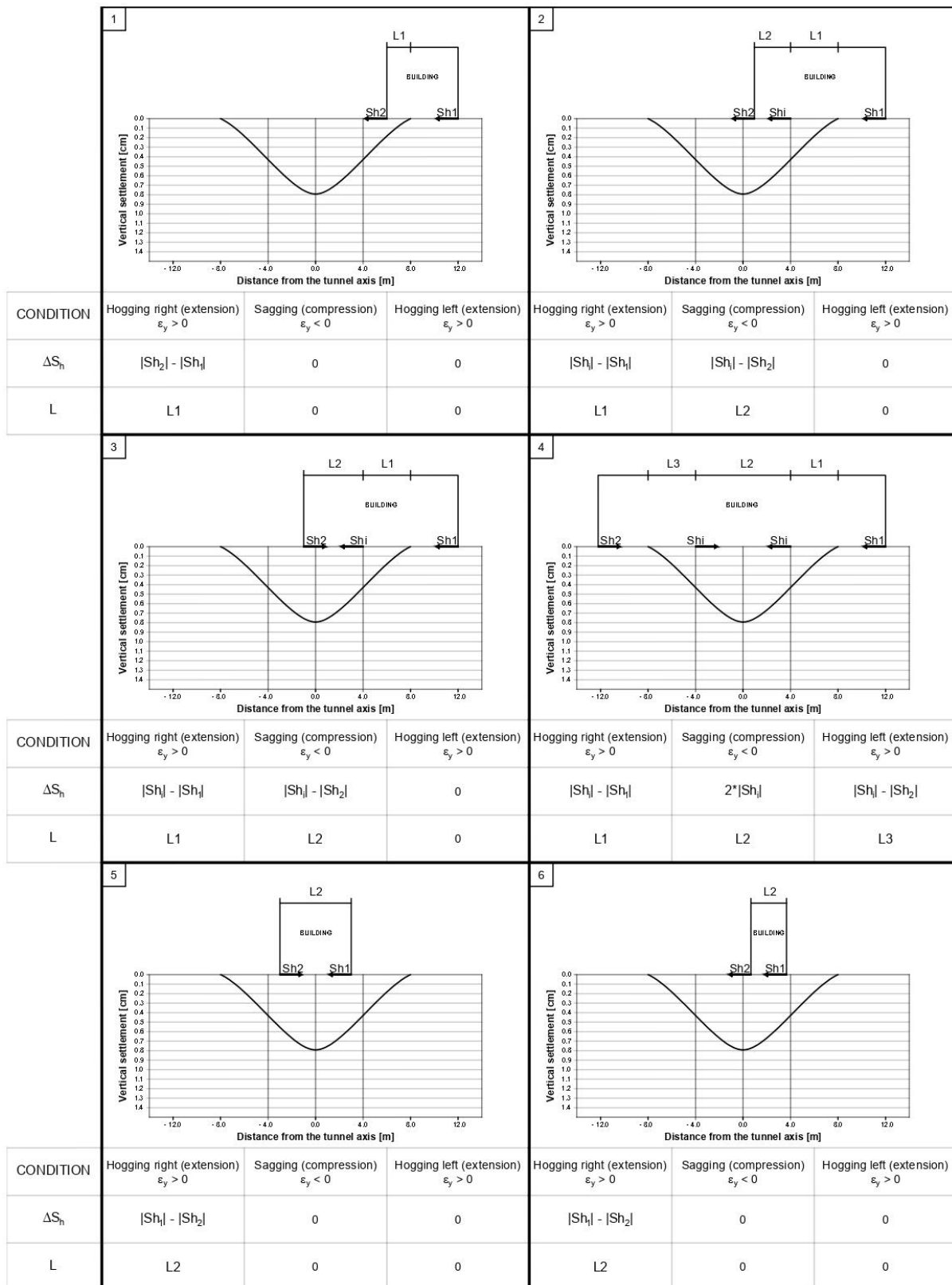


Figure 13 Sign of the horizontal displacement

Once calculated the horizontal strain, it is possible to compute the two overall tensile strains (ε_t) by the next equations:

$$\varepsilon_t = \varepsilon_{b_max} + \varepsilon_h$$

$$\varepsilon_t = \frac{\varepsilon_h}{2} + \sqrt{\left(\frac{\varepsilon_h}{2}\right)^2 + \varepsilon_{d_max}^2}$$

The final step is to compare the maximum overall tensile strain with the threshold tensile strain proposed by Burland (1977) in the table below (Table 2).

Table 2 Damage classification (Burland, et al., 1977)

Category of risk of damage	Degree of severity	Description of typical damage	Crack width [mm]	Control parameter (tensile strain) ε_{lim} [%]
0 aesthetic	Negligible	Hairline cracks	<0.1	0–0.05
1 aesthetic	Very slight	Fine cracks which are easily treated during normal decoration. Damage generally restricted to internal wall finishes. Close inspection may reveal some cracks in external brickwork or masonry.	<1.0	0.05–0.075
2 aesthetic	Slight	Cracks easily filled. Redecoration probably required. Recurrent cracks can be masked by suitable linings. Cracks can be visible externally and some repointing may be required to ensure watertightness. Doors and windows may stick slightly.	<5.0	0.075–0.15
3 aesthetic/functional	Moderate	The cracks require some opening up and can be patched by a mason. Repointing of external brickwork and possibly a small amount of brickwork to be replaced. Doors and windows sticking. Service pipes may fracture. Watertightness often impaired.	5–15 (many crack with width >3 mm)	0.15–0.3
4 functional/serviceability	Severe	Extensive repair work involving breaking-out and replacing sections of walls, especially over doors and windows. Windows and door frames distorted, floor sloping noticeably. Walls leaning or bulging noticeably, some lose of bearing in beams. Service pipes disrupted.	15–25 (but depend on the number of cracks)	>0.3
5 structural	Very severe	Major repair job involving partial or complete rebuilding. Beams lose bearing, walls lean badly and require shoring. Windows broken with distortion. Danger of instability.	>25 (but depend on the number of cracks)	

For the reinforced concrete buildings or isolated foundations, Rankin (1988) proposes a classification focusing on the maximum angular distortion β_{max} coupled with the maximum settlement S_{max} . The maximum angular distortion is in function of the vertical settlement of every single footing (S_i) and their spacing (L_i), as shown in the Figure 14.

$$\beta_{max} = \frac{(S_i - S_{i-1})}{L_i}$$

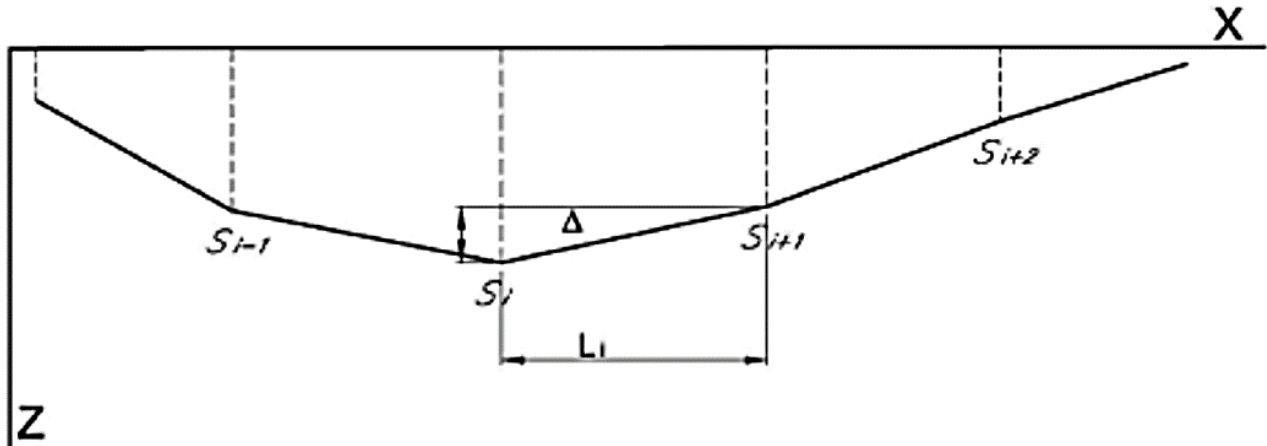


Figure 14 Settlement under a reinforced concrete building

Threshold values of the maximum angular distortion β_{max} and the maximum settlement S_{max} are reported in the Table 3 below.

Table 3 Damage classification (Rankin, 1988)

Category of risk of damage	Degree of severity	Description of typical damage	Control parameters	
			β_{max}	S_{max} [mm]
1 Aesthetic	Negligible	Superficial damage unlikely.	<1/500	<10
2 Aesthetic	Slight	Possible superficial damage which is unlikely to have structural significance.	1/500–1/200	10–50
3 Functional	Moderate	Expected superficial damage to buildings and expected damage to rigid pipelines.	1/200–1/50	50–75
4 Service-ability and structural	High	Expected structural damage to buildings and damage to rigid pipelines; possible damage to other pipelines.	>1/50	>75

It is important to highlight that both the classifications are valid for good-condition buildings, however, if a construction is already damaged, some correction factors are introduced.

Chiriotti et al. adjusted Rankin and Burland thresholds considering the vulnerability index. These new values are more stringent and more precautionary from the point of view of safety. The Table 4 and Table 5 shows the new thresholds for Burland and Rankin, respectively.

Table 4 New Burland damage classification (Chiriotti, et al., 2000)

Category of damage	Vulnerability index I_v of the building									
	Negligible		Low		Slight		Medium		High	
	$0 < I_v < 20$		$20 < I_v < 40$		$40 < I_v < 60$		$60 < I_v < 80$		$80 < I_v < 100$	
	Reduction factor F_R									
	$F_R = 1.0$		$F_R = 1.25$		$F_R = 1.50$		$F_R = 1.75$		$F_R = 2.0$	
	Control parameter									
	ε_{lim} [%]		ε_{lim} [%]		ε_{lim} [%]		ε_{lim} [%]		ε_{lim} [%]	
	min.	max.	min.	max.	min.	max.	min.	max.	min.	max.
0	0,000	0,050	0,000	0,040	0,000	0,033	0,000	0,029	0,000	0,025
1	0,050	0,075	0,040	0,060	0,033	0,050	0,029	0,043	0,025	0,038
2	0,075	0,150	0,060	0,120	0,050	0,100	0,043	0,860	0,038	0,075
3	0,150	0,300	0,120	0,240	0,100	0,200	0,860	0,171	0,075	0,150
4 to 5	>0,300		>0,240		>0,200		>0,171		>0,150	

Table 5 New Rankin damage classification (Chiriotti, et al., 2000)

		Vulnerability index I_V of the building									
		Negligible		Low		Slight		Medium		High	
Category of damage		$0 < I_V < 20$		$20 < I_V < 40$		$40 < I_V < 60$		$60 < I_V < 80$		$80 < I_V < 100$	
		Reduction factor F_R									
		$F_R = 1.0$		$F_R = 1.25$		$F_R = 1.50$		$F_R = 1.75$		$F_R = 2.0$	
		Control parameter									
		S_{max} [mm]	β_{max}	S_{max} [mm]	β_{max}	S_{max} [mm]	β_{max}	S_{max} [mm]	β_{max}	S_{max} [mm]	β_{max}
1		<10	<1/500	<8	<1/625	<6,7	<1/750	<5,7	<1/875	<5	<1/1000
2		10–50	1/500– 1/200	8–40	1/625– 1/250	6,7–33	1/750– 1/300	5,7–28,5	1/875– 1/350	5–25	1/1000– 1/400
3		50–75	1/200– 1/50	40–60	1/250– 1/63	33–50	1/300– 1/75	28,5–43	1/350– 1/88	25–37,5	1/400– 1/100
4		>75	>1/50	>60	>1/63	>50	>1/75	>43	>1/88	>37,5	>1/100

Once the vulnerability index and the damage category are defined, a risk matrix can be built, as shown in the Figure 15. It has on the y-axis the vulnerability index and on the x-axis the damage category. Hence, by combining this two information it is possible to define the risk related to each building expressed by a colour:

- Green: the potential damage is negligible or slight and the building is in good condition;
- Yellow: the induced damage on the building are negligible or slight, but due to its condition a standard monitoring is needed during the excavation;
- Orange: the effects of the excavation on the building could induce damage and so a detailed monitoring program must be selected;
- Red: the risk is high because of the amount of the induced deformation, hence in addition to the detailed monitoring system a ground improvement treatments, as countermeasures, are designed.

		Vulnerability index				
		Negligible $0 < I_v < 20$	Low $21 < I_v < 40$	Slight $41 < I_v < 60$	Medium $61 < I_v < 80$	High $81 < I_v < 100$
Degree of induced damage	Negligible 0 - 1					
	Slight 2					
	Moderate 3					
	Severe 4 - 5					

Figure 15 Risk matrix

Consequently, it is possible to identify a flowchart composed by several steps in order to define the risk of tunnelling-induced damages:

1. Identification of the control parameters;
2. Determination of the threshold limit value for the selected control parameters;
3. Evaluation of the ground movement and of the influence zone;
4. Realization of the settlement sensitivity analysis for all the building within the influence zone through the abovementioned BCS and BRA;
5. Comparison between the computed surface displacement and the results of the sensitivity analysis and identification of the category of risk;
6. Drafting of a Ground Movement Analysis Report;
7. Individuation of the buildings at risk
8. Definition of the risk management strategy.

4. THREE-DIMENSIONAL FEM ANALYSIS WITH MIDAS FEA NX

The aim of this chapter is to analyse all the steps, which characterize the 3D numerical modelling, from the selection of the input data to the creation of the 3D model. The numerical simulations are done with the software 3D Midas FEA NX with the aim to evaluate the surface settlements induced by the excavation.

4.1. Geological and geotechnical characterization of the site

The studied sections of the tunnel alignment go from the chainage 6694 m to 7040 m in order to analyse the passage from an offset arrangement of the twin tunnels with an angle of 30° to the piggyback one where they are perfectly overlapped, as shown in the Figure 16.

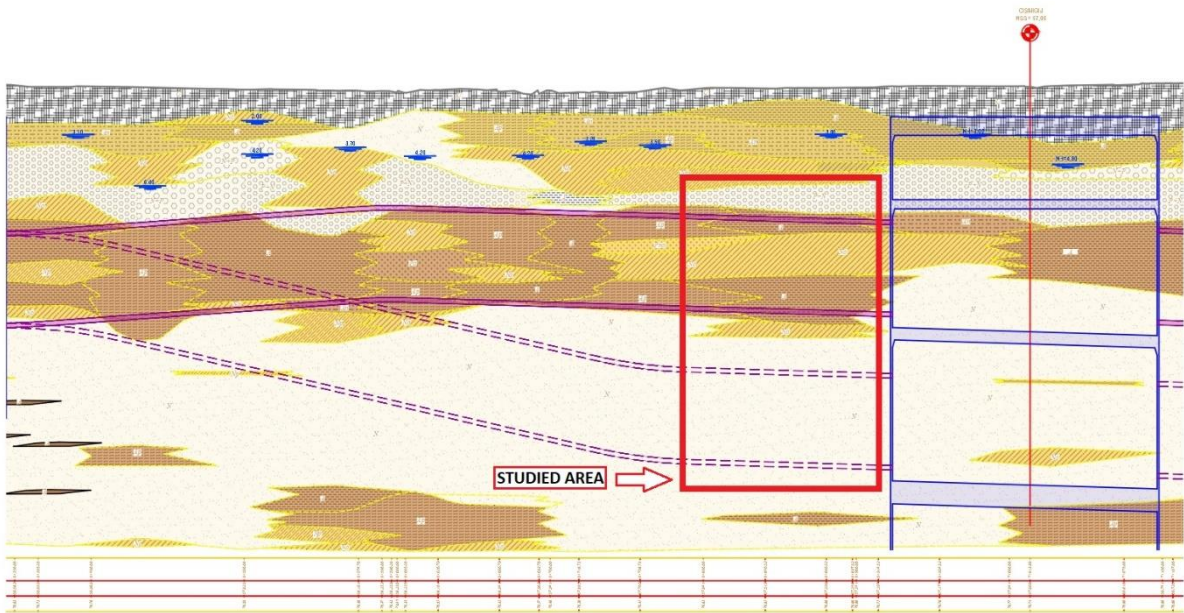


Figure 16 Longitudinal section of the studied area

In the studied zone of about 346 m in length, it is possible to define seven geological units of soil thanks to several core-drilling surveys already realised in this area. The geological units are defined below, as reported in the Figure 17:

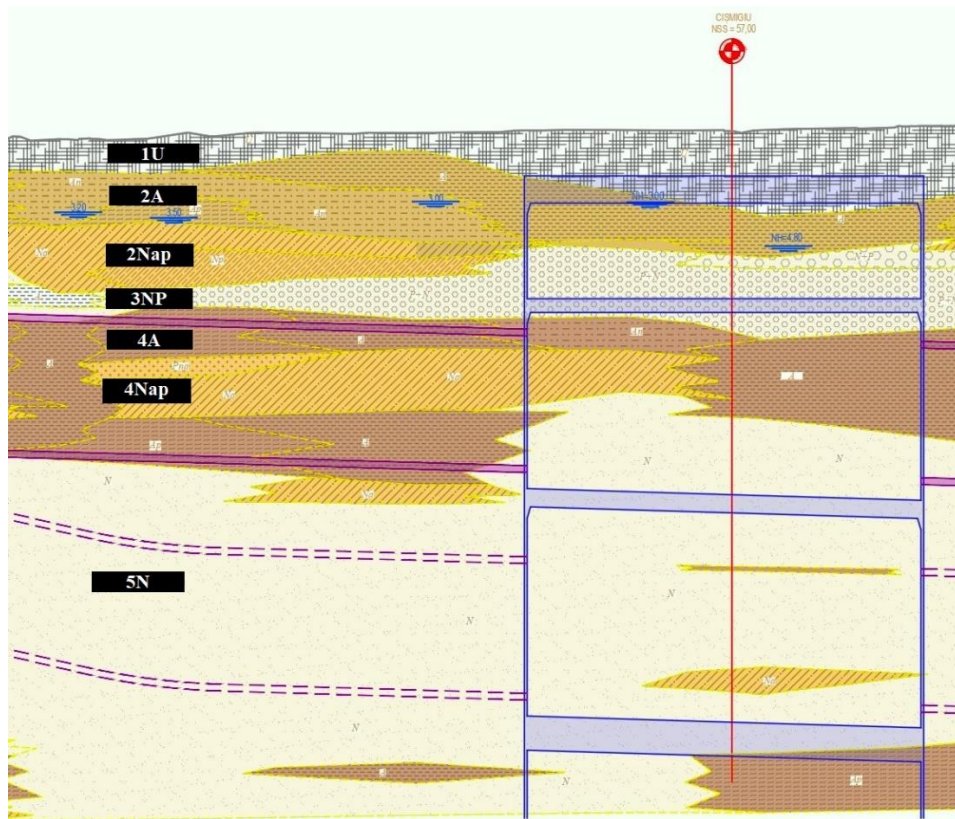


Figure 17 Stratigraphy of the studied area

1. Anthropogenic filling and vegetal soil (1U);
2. Upper clay-sandy complex characterised by Holocene deposit of loess, clay and sand (2A);
3. Colentina gravel complex is the carrier complex of the Colentina aquifer and contains gravel and sand with a variable granulometric distribution (2Nap);
4. Intermediate clay layer containing up to 80% consolidated hard clay and limestone concretions with thin sand lenses and interspersed dusty earths (3NP);
5. The sands of Mostiștea, the carrier formation of the Mostiștea aquifer, is a layer of sand with medium and fine grain sands (4A);
6. The lacquer complex, composed of a variation of marnous clay, limestone and fine sands, the grain $< 0,005$ mm constituting approximately 86 % (4Nap);

7. Fratesti complex or lower complex of gravel, bearing the "Fratesi aquifer", is discordant on layers of leachocene levantine clay. This complex comprises three thick layers of sandy gravel, separated by two horizons of marl or clay (5N).

The properties of the identified layers are listed in the Table 6.

Table 6 Geomechanical parameters of the layers

Layer code	Thickness [m]	γ [kN/m ³]	E [kN/m ²]	c' [kN/m ²]	ϕ [°]	k_0 [-]	k [m/s]
1U	1.5	18	8000	1	20	0.53	1.0E-09
2A	2.5	20	11000	40	17	0.50	1.0E-09
2Nap	2	20	11000	5	20	0.49	1.0E-05
3NP	2	21	20000	0	28	0.49	1.0E-04
4A	1.5	20	15000	55	16	0.43	1.0E-09
4Nap	3	20	15000	5	25	0.49	1.0E-05
4A	3	20	15000	55	16	0.43	1.0E-09
5N	29.5	21	25000	0	30	0.49	1.0E-04

Under the point of view of the hydrological condition, the water table is shallow due to the presence of the Dambovita River and in particular can be fixed at three meters under the ground surface. Moreover, under the point of view of hydraulic conditions, the layers 1U, 2A and 4A are undrained: this behaviour is highlighted in the Table 6 looking at the hydraulic conductivity (k), which has a very low value for these strata.

In this work, only the worst arrangement is considered due to huge size of the model and so, the piggyback layout is analysed, which represents the zone of the pathway of the metro line approaching and passes through the station (from

6980m to 7040m). It is chosen as the worst condition because the tunnels are very close ($0.5 \cdot D$) and this aspect produces an important mutual effect between them and the maximum surface settlement.

4.2. Creation of 3D geometry

The first step of modelling is the creation of 3D geometry. The software FEM “Midas FEA NX” allows to create very complex geometric objects thanks to the presence of the latest generation of 3D geometric modelling tools.

The created elements are listed below:

- Three parallelepipeds that represent the layered soil;
- Two cylindrical elements depict the twin tunnels, which are subsequently subdivided in 1.5 m-long units thanks to surfaces in order to define the different construction steps;
- Six circular crown shaped solids to figure out the annular voids, which will become the grout, the linings and the shield also divided as before;
- Two cylindrical lateral surfaces that identify a fictitious element, placed inside the lining.

Taking a closer look to the layered soil, the stratigraphy is characterized by eight strata, but in order to simplify the model, the layers 4A, 4Nap and again 4A are melted together. The new element has the geomechanical properties of the 4Nap because it represents the worst situation due to its drained condition. The same operation is done for the layers 1U, 2A, 2Nap and 3NP choosing a drained hydraulic condition even if some of them are undrained, as shown in the Table 6.

About the structural elements, the following geomechanical parameters are selected (Table 7):

Table 7 Mechanical parameters of the structural elements

STRUCTURAL ELEMENT	MODEL BEHAVIOUR	UNIT WEIGHT [kN/m ³]	MODULUS OF ELASTICITY [MPa]	POISSON RATIO [-]
SHIELD OF THE EPB	Isotropic – Elastic	24	209	0.15
PRECAST CONCRETE LINING	Isotropic – Elastic	23.53	35000	0.2
GROUT (Shah, et al., 2017)	Isotropic – Elastic	24	2000	0.3

Moreover, about the position in the space of the twin tunnels, six sections of the project are investigated. From them, a series of coordinates, changing the chainage, for both the tunnels are extrapolated, as shown in the Table 8 below.

Table 8 Studied chainage and relative tunnels coordinates

CHAINAGE [m]	TUNNEL 1			TUNNEL 2		
	x [m]	z [m]	y [m]	x [m]	z [m]	y [m]
6+980	0	23	40	0	33	40
7+000	0	23	60	0	33	60
7+020	0	23	80	0	33	80
7+040	0	23	100	0	33	100

Once the coordinates are defined, the three dimensions of the model must be established. The model must be enlarged in order to avoid boundary effects due to the presence of the boundary conditions. In particular, the width is fixed at 120 m and the depth at 45 m, as reported in Figure 18.

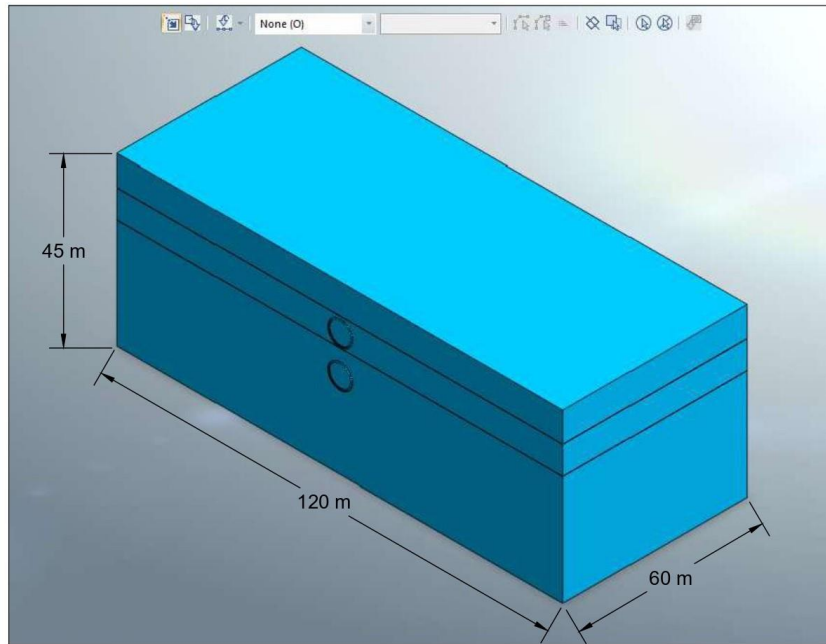


Figure 18 Dimensions of the model

The last step for the setting up of the geometry is the function “Auto Connect”. It automatically creates a shared face between objects (MIDAS, 2021). In addition, in case of solids partially or totally included each other, as in the current situation, this function is able to solve the inclusion by cutting the host object: the parallelepiped is cut to host the cylinder.

4.3. Mesh generation

A mesh is defined as a structural build of a 2D or 3D model consisting of polygons. In this specific case, the software Midas FEA NX gives to the user the opportunity to select two different shapes of polygons, as the tetrahedral elements and the hybrid one (combination between the hexahedral and pyramidal elements), in order to manage better the model.

The procedure to define completely the mesh is explained as follow:

1. Materials definition;
2. Properties selection;
3. Size control;
4. 2D and 3D Mesh generation;
5. Rename;
6. Change property.

The first step is the definition of the materials in the *Material* menu (Figure 19) of all the abovementioned geometrical elements. To do that, it is important to select the right model, which best approximates the real behaviour of the materials. These constitutive models are selected based on a laboratory tests campaign and a data processing already done before the modelling activity by the Systra SWS, the company at which the M5 project is entrusted. The Hardening Soil model is chosen for the layered soil because it is more suitable for the settlement calculation, while for the grout, the shield and the lining a linear elastic model is more suitable. For both the isotropic models, all the main parameters must be inserted in order to define the stiffness and the initial condition of the material.

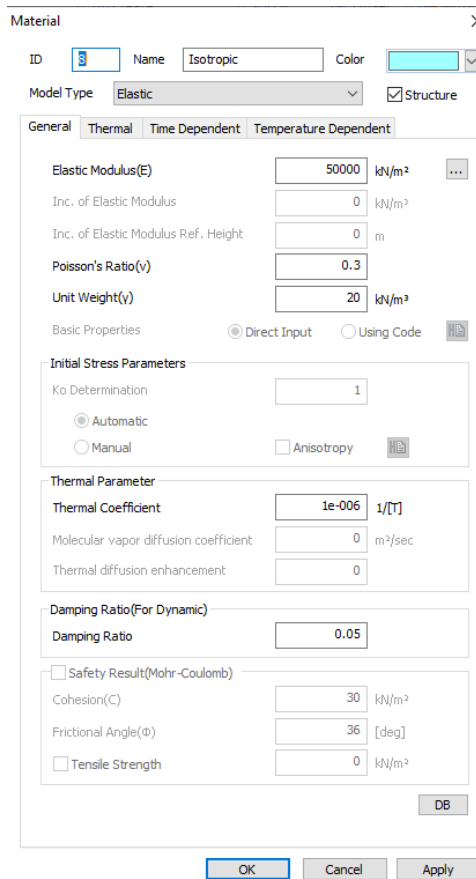


Figure 19 Material menu

The second step is to define the properties for ground and for structural elements. It means that, based on the type of geometrical element, solid or shell in this work, it is possible to assign 3D (only determination of the material) or 2D properties (determination of the material and the size) thanks the Property menu in Figure 20.

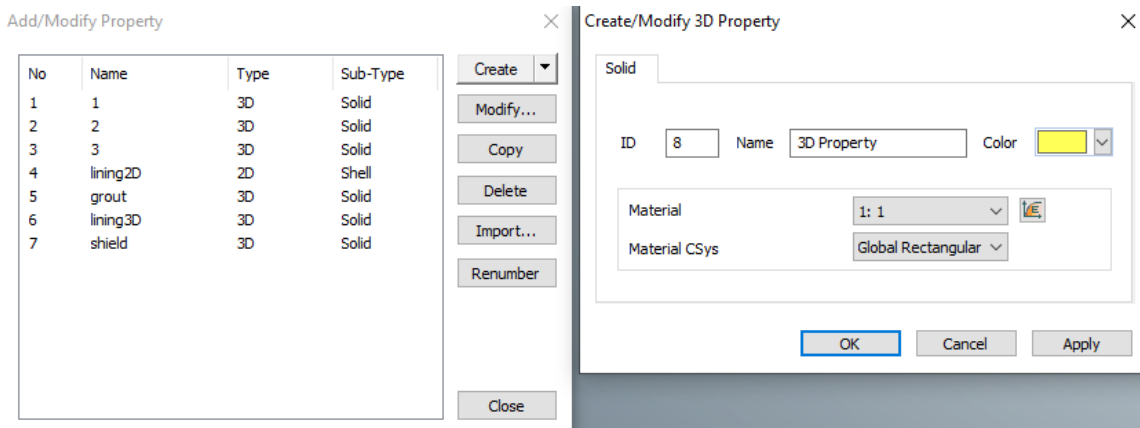


Figure 20 Property menu

The third step is the specification of the size of the element mesh surrounding a point. The *Size Control* command (Figure 21) is useful to thicken the mesh for results that are more accurate and vice versa. The software does this automatically.

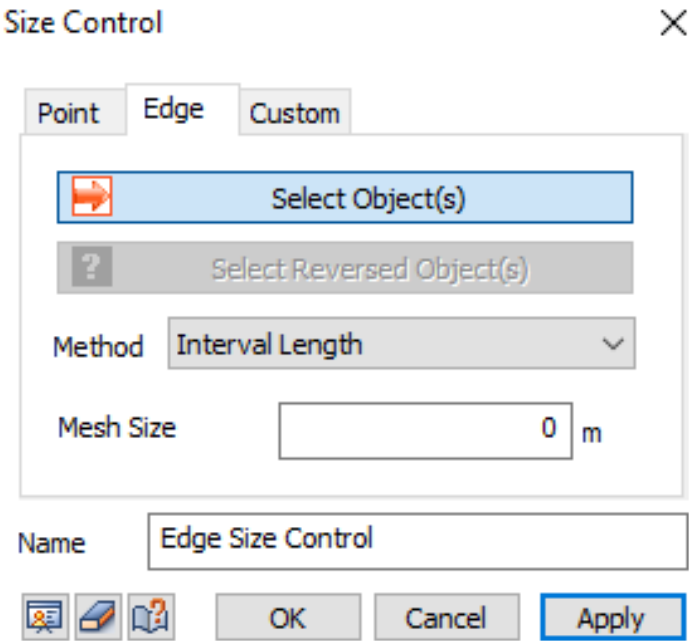


Figure 21 Size Control menu

The fourth step is the generation of the mesh, task that the software does automatically by the *Auto-Face* function for two-dimensional elements and the *Auto-Solid* function for three-dimensional ones, as reported in the Figure 22. For both of them, it is necessary to specify only the mesh size and the property of the geometry on which the program creates the mesh. An additional option for the 3D function is to select the shape of mesh.

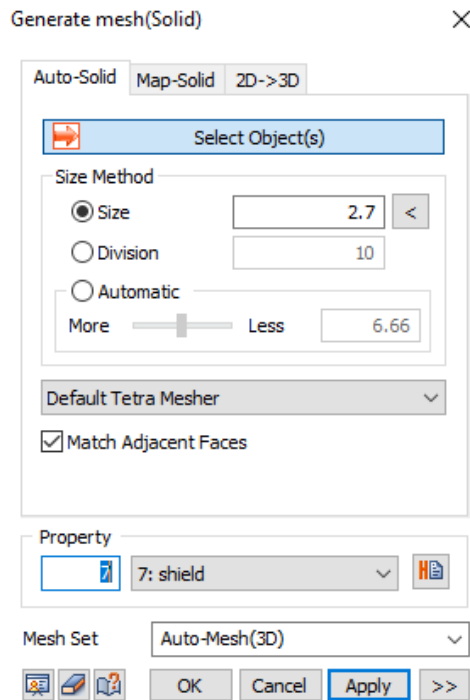


Figure 22 Mesh menu

The fifth step is the *Rename* (Figure 23). It means that every mesh set can be renamed and so sorted based on the coordinate system. This operation is extremely important because the *Auto-Mesh* functions do not respect the order of the geometrical elements imposed by the coordinate system.

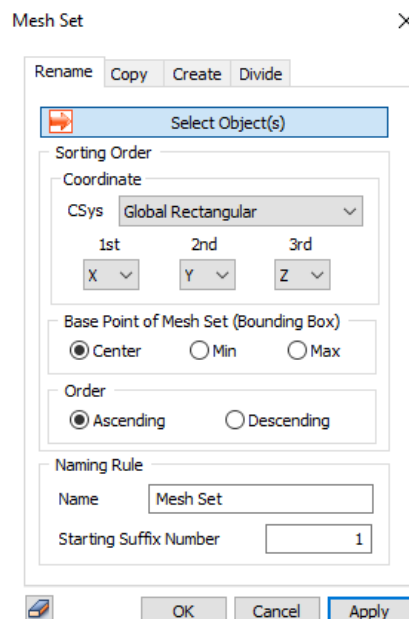


Figure 23 Rename menu

The last step is the addition to the mesh set another property of material if the original one change during the analysis (i.e. one geometrical element at the beginning is ground and then becomes shield). The command used is *Change Property* (Figure 24), where after the selection of the mesh set, simply a specific property is chosen. This operation creates a new set of boundary condition for the selected objects.

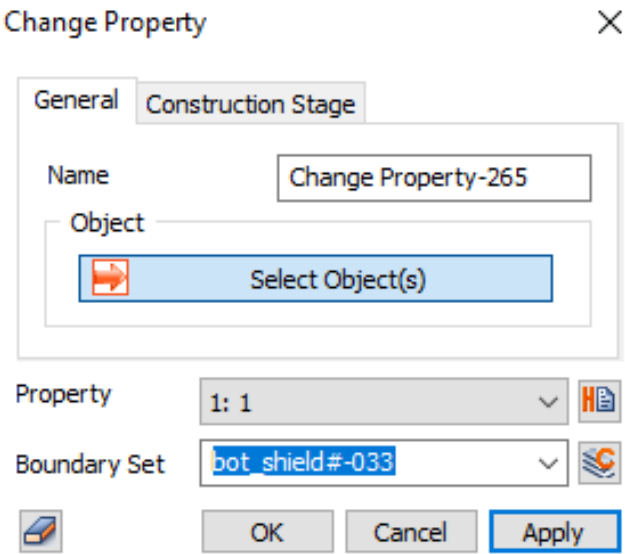


Figure 24 Change Property menu

After this procedure, all mesh sets are ready for the next operations.

4.4. Static Analysis

In this phase of modelling, the initial condition, the boundary condition and the load sets can be assigned.

4.4.1. Static conditions input

In order to simulate the real condition of the ground two fundamental commands must be used: the *Constraint* and the *Self Weight*.

The command *Constrain* automatically sets the constraint conditions all around the model. The displacement along x direction is locked for the left and right side. For the front and back sides, the displacement along y-direction is

constrained. Finally, the displacement along both x and y direction is prevented for the bottom side.

The *Self-Weight* command automatically sets the self-weight of the whole model simply by selecting the axis and the direction along which it must be applied.

4.4.2. Load condition and its calculation

The loads play a key role for a correct simulation of a model. In this study, the inserted pressures are the face pressure, the radial one along the shield and the radial one due to the grout injection.

The loads can be inserted in the model thanks to the command *Pressure*. The pressures will be applied on the entire element face in uniform way. In addition, the direction of the pressure can be set by selection of one of the available possibilities offered in this menu.

However, before the pressures input in the software, the crucial point is their evaluation. The main assumption is that all layers of the ground are in drained condition, as mentioned before: this is not the real behaviour, but it represents the worst condition for the excavation at short term.

Afterward, Anagnostou and Covari method is used to compute the face stability pressure at the tunnel axis. This theory can be applied only in drained condition and with homogeneous soil (Anagnostou, et al., 1996). Nevertheless, in the present case, the soil is characterised by seven layers with completely different geomechanical properties. Hence, the first step is to find the equivalent parameters for the entire medium. With this purpose, the theory of Loganathan and Poulos is used: the equivalent mechanical parameters are computed by the weighted average based on the thickness of the layers (t) and the vicinity to the excavation. This second condition is controlled by the “W” parameter that

changes its value by changing the distance from the tunnel. The formula and the calculation scheme are reported below (Figure 25):

$$Parameter_{eq} = \frac{\sum_{i=1}^n t_i * w_i * Parameter_i}{\sum_{i=1}^n t_i * w_i}$$

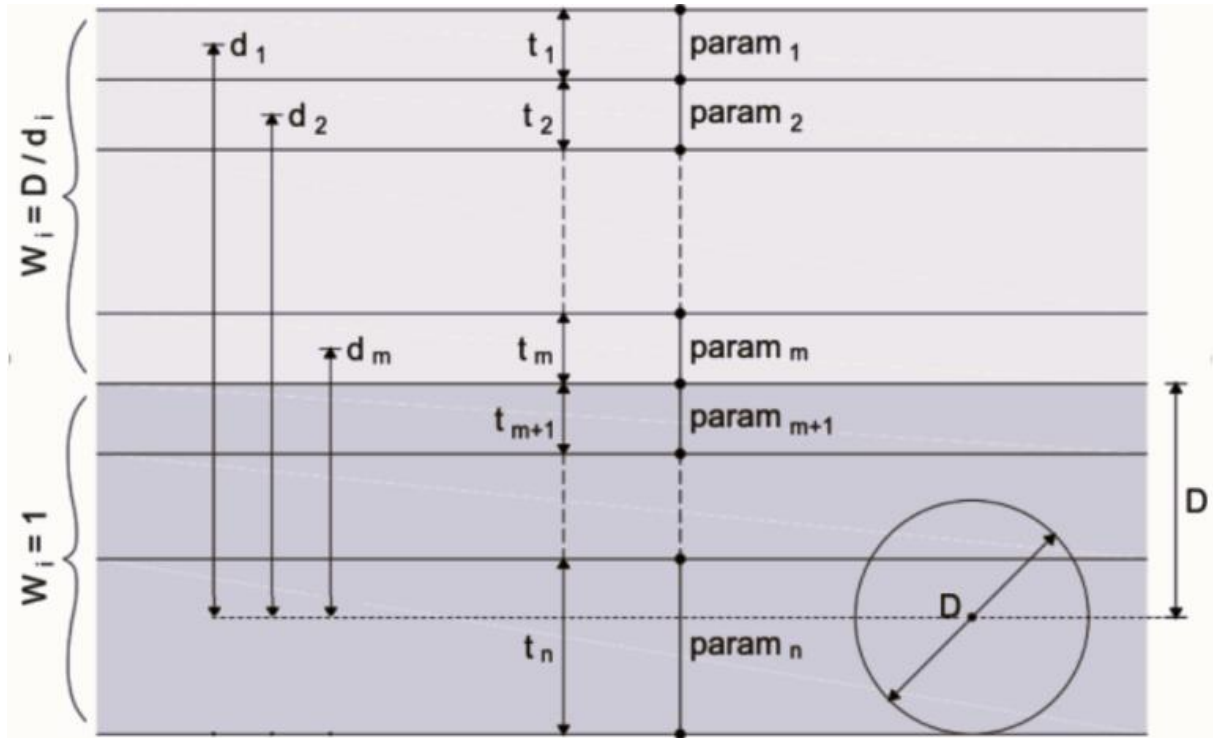


Figure 25 Scheme used for the equivalent parameter computation

The Table 9 figures out the equivalent parameters computed:

Table 9 Equivalent parameter for the pressure calculation

Tunnel position	$\gamma_{equivalent}$ [kN/m ³]	$C_{equivalent}$ [kN/m ²]	$\phi_{equivalent}$ [°]	$k_{0,equivalent}$ [-]
UPPER TUNNEL	20.0	9.6	22.9	0.5
BOTTOM TUNNEL	20.6	3.6	27.2	0.5

Once all the equivalent parameters are calculated for all the depths, the Anagnostou and Covari formula can be applied:

$$S_{A\&K} = F_0 * \gamma'_{eq} * D - F_1 * c_{eq} + F_2 * \gamma'_{eq} * \Delta h - F_3 * c_{eq} * \frac{\Delta h}{D}$$

where:

- F_0, F_1, F_2, F_3 are the dimensionless coefficients reported in the Figure 26;
- γ'_{eq} is the equivalent submerged unit weight;
- c_{eq} is the equivalent cohesion;
- D is the diameter of the tunnel;
- $\Delta h = (h_0 - h_f)$ is taken equal to zero.

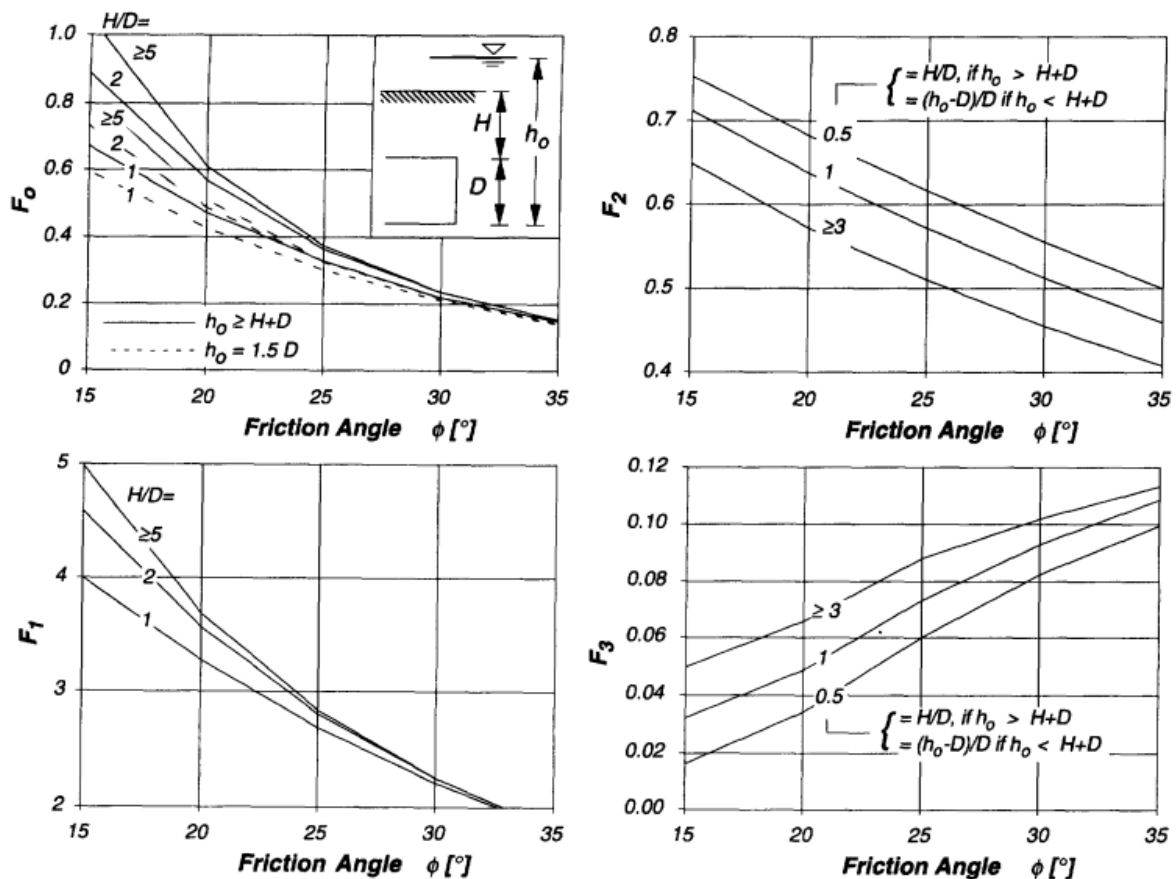


Figure 26 Anagnostou & Covari nomograms

Moreover, at this pressure, the water load must be added and in order to obtain the design pressure some safety factors are included:

$$s' = S_{A\&K} * 1.5 + \gamma_{water} * \left(h_0 - \frac{D}{2} \right) * 1.1$$

The result of this equation is the minimum pressure that the Tunnel Boring Machine must apply in order to guarantee the face stability.

Another pressure has to be defined, the maximum pressure that must never be exceeded to prevent the blow-up of the soil and the blow-out of the foaming agent. This pressure can be calculated thanks to the following equation (DAUB, 2016):

$$\sigma_{v,axis} = 0.9 * \left(\gamma_{eq} * H + \gamma_{conditioned\ soil} * \frac{D}{2} \right)$$

In this formulation, the unit weight of the conditioned soil is taken equal to 14 kN/m³.

The maximum pressure has to be compared with maximum pressure that the machine is able to apply.

Once the minimum and maximum pressures are computed for both tunnels, an operational pressure value for the machine can be selected. The chosen values are 135 kPa and 225 kPa for the tunnel 1 and tunnel 2, respectively.

4.5. Stage Wizard

The only way to simulate the excavation process is to set up a wizard thanks to the *Stage Wizard* command. In this menu, it is possible to activate or deactivate one or more elements, as meshes, loads and boundary conditions in a specific order to build all the construction stages. The simulated excavation processes

are two: the upper tunnel excavated as first and the bottom tunnel excavated as first.

The first step is the design of the *Initial Stage* in which the initial hydraulic, geotechnical and boundary conditions are specified.

Moreover, the rules of the construction stage must be assigned based on:

- Mesh set type: it possible to choose the type of set to add between meshes, loads and boundary conditions;
- Set Name Prefix, in which there are the set names that must be inserted;
- A/R means that elements can be activated or removed;
- Start Postfix is the numerical code from which a set must be added;
- End Postfix specifies if a set must be added up to a certain number;
- Postfix Increment: input the number increment used as the construction stage progresses;
- Start Stage: fix the first stage number from where starting;
- Stage increment: select the increment in stage that must be used.

To better clarify the mesh sets added in the construction stage rules, in the Figure 27 and Figure 28 below, the names of them are highlighted.

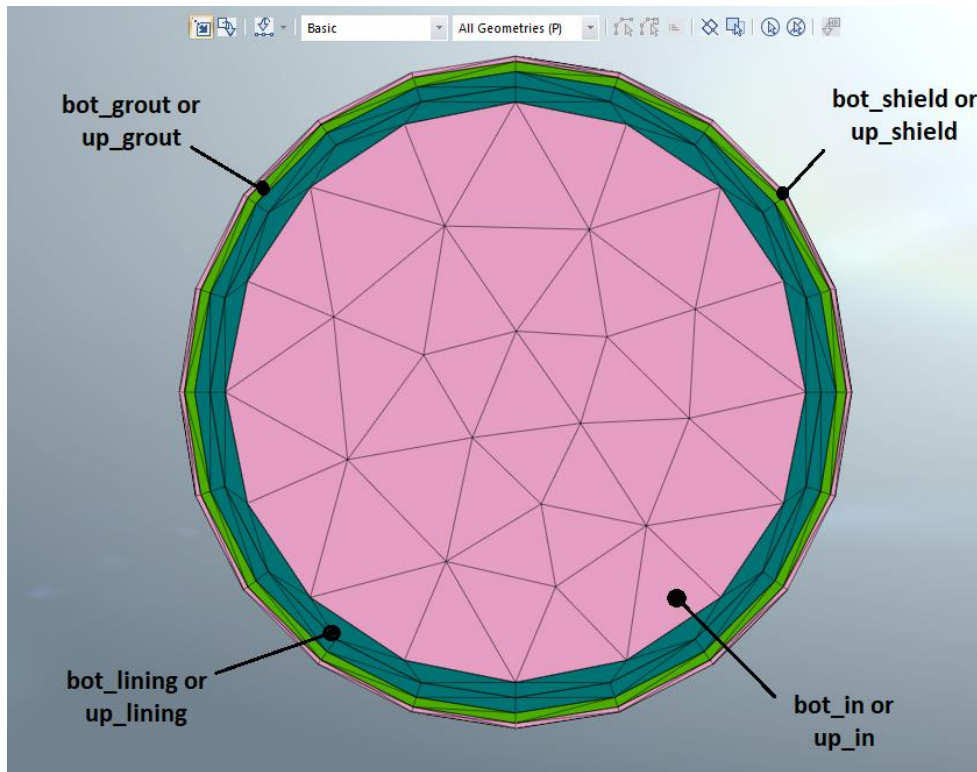


Figure 27 Names of the mesh sets for the tunnel

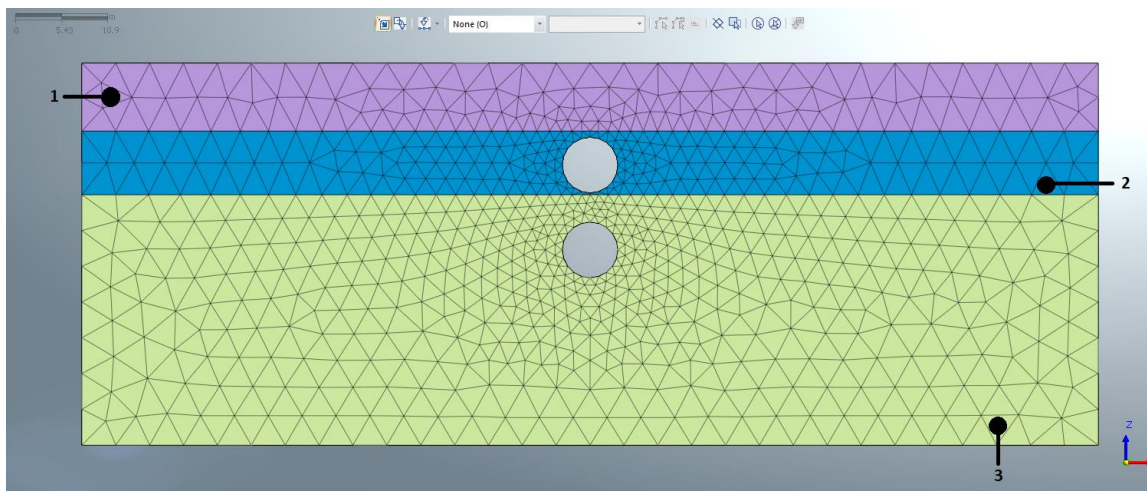


Figure 28 Names of the mesh set for the soils

In particular, the rules for the first excavation process applied in the model are shown in Figure 29 and summarised as follow:

- Stage 1: deactivation of the first up_in, up_grout, and up_lining mesh sets, activation of the first upper shield with its boundary condition and activation the first face pressure FU related to the upper tunnel ;

- Stage 9: activation of the first upper lining and grout and their change property boundary conditions and deactivation of the pressure and the first shield;
- Stage 42: deactivation of the first bot_in, bot_grout, and bot_lining mesh sets, activation of the first bottom shield with its boundary condition and activation the first face pressure FB related to the bottom tunnel;
- Stage 50: activation of the first bottom lining and grout and their change property boundary conditions and deactivation of the pressure and the first shield;
- The other stages are automatically fixed by the program as a combination of the previous two stages.

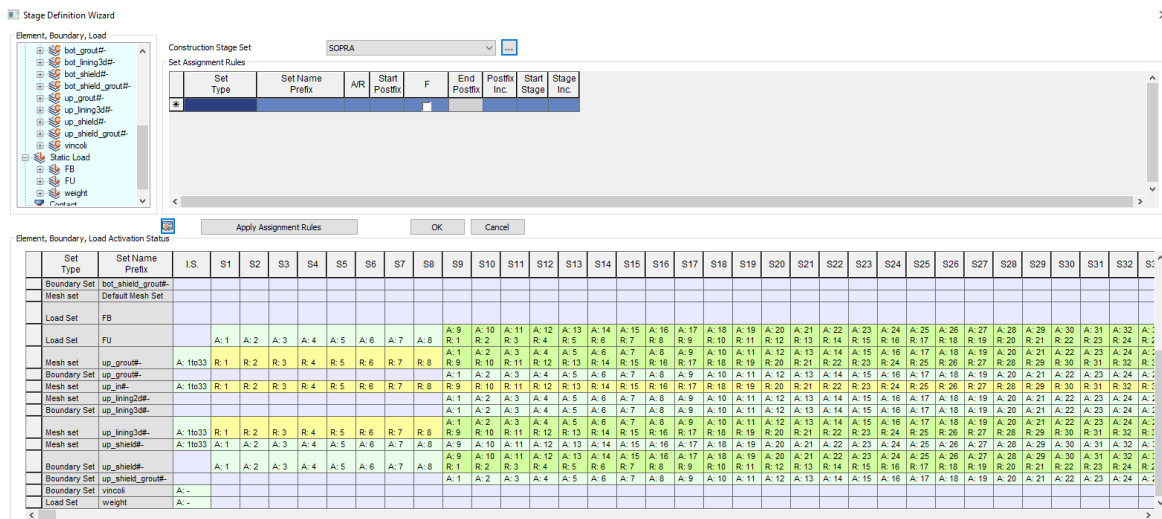


Figure 29 Stage Wizard definition

These rules simulate the excavation of the soil by the EPB machine, the application of the pressure able to stabilise the face front, the advancement of the machine, the installation of the lining and the injection of the grout to fill the annular gap for both the tunnels.

The rules applied for the excavation of the bottom tunnel as first are the same but inverted.

5. TWO-DIMENSIONAL FEM ANALYSIS WITH PLAXIS 2D

PLAXIS2D is a two-dimensional FEM software. The first difference with the 3D is that it is possible to draw, analyse and study planar sections. Even if the longitudinal component is not considered, it is possible to simulate the three dimensionality of the problem, analysing different transversal sections or applying an internal radial pressure, e.g. at the face front of the tunnel or when the lining is installed. The advantages of 2D FEM analysis are the easier creation of the model and the faster velocity on the calculations. This allows, if necessary, the change of some parameters in a short time.

Initially three different arrangements of the tunnels are analysed, resuming the initial project of the Bucharest metro line: horizontal, offset and vertical layouts. After that, a second different analysis is performed considering only the piggyback configuration, which is the most particular and unusual one.

5.1. Geometry of the model and mesh generation

The stratigraphy is considered with its different soil layers, as reported in Figure 30; hence, no simplification is made, differently to the 3D model. The sizes of the 2D model are taken as those of the 3D one, in particular 120 meters in length and 45 meters in height. In PLAXIS2D, it is possible to define the stratigraphy describing the layers of a virtual borehole. In practice, the characteristics like thickness, physical and geo-mechanical parameters are inserted and automatically assigned to the previous defined dimensions of the model. At this step, the water-head is inserted.

The Figure 30 shows the screen of PLAXIS2D for the definition of soil properties.

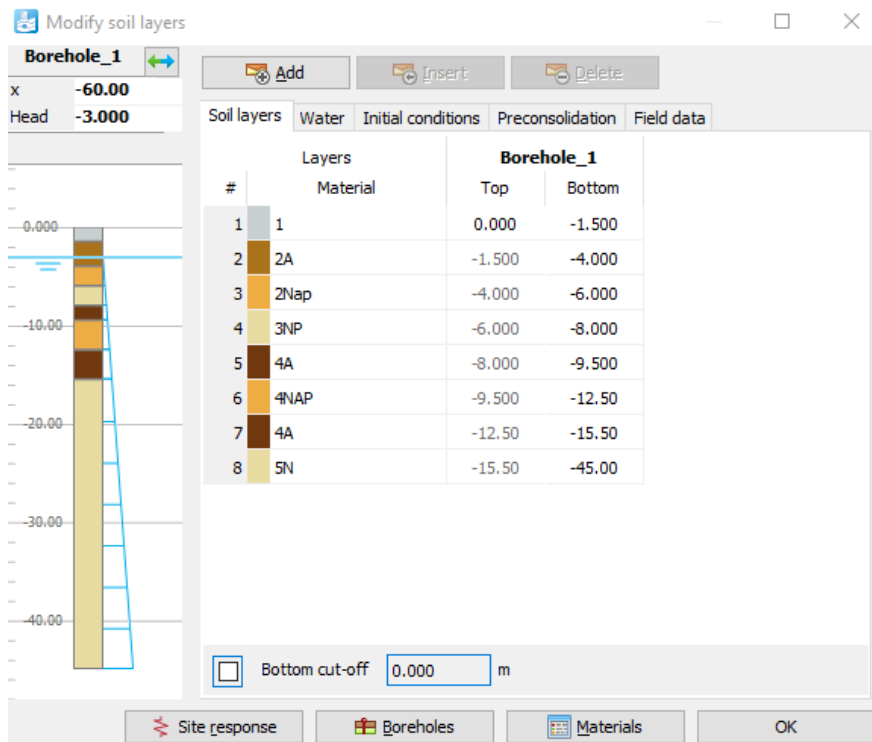


Figure 30 Borehole definition

The tunnel linings are modelled as plate, with the parameters of the segment reinforced concrete reported in the Table 7. An important step is the creation of interfaces, which allow the interaction between the tunnel lining and the soil. In this way, two nodes are created (Figure 31), one regards the soil and the other the structure: the interaction is like elastic-perfectly plastic springs.

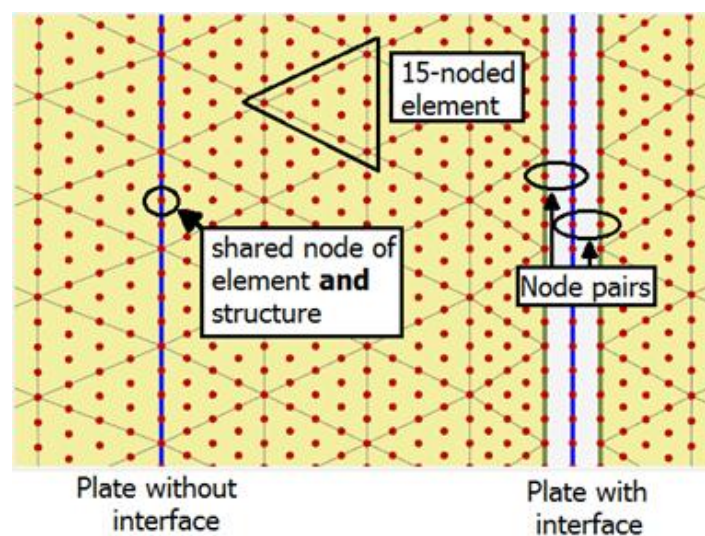


Figure 31 Interfaces

In this model, the external diameter of the lining is equal to 6.6 meters, equal to the excavation diameter, since the shield and the grout are not simulated in 2D models.

The studied configurations are below summarised showing the geometrical parameters and the figures of 2D models.

Horizontal configuration (Figure 32):

- Axis depth: 13 meters;
- Horizontal inter-axis distance : 13.6 meters;

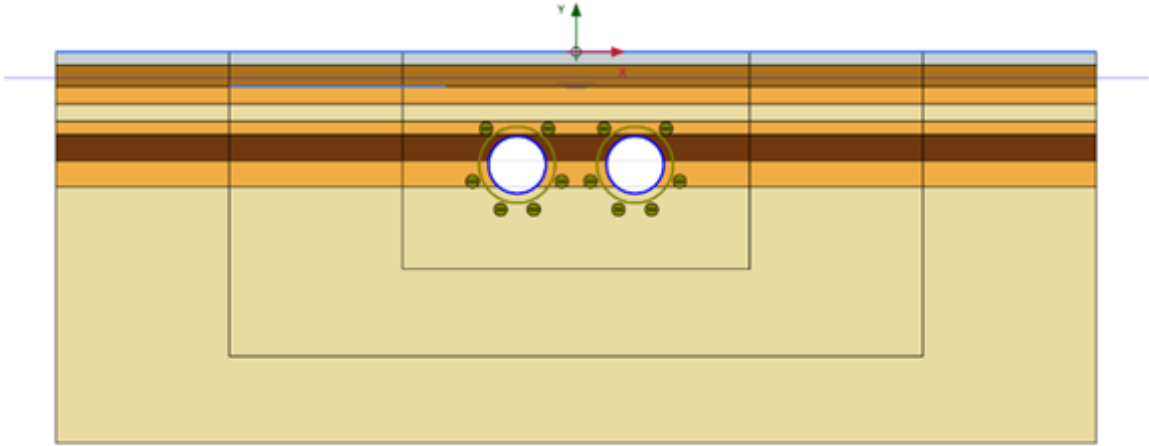


Figure 32 Horizontal configuration

Offset configuration (Figure 33):

- Axis depth tunnel right: 12 meters;
- Axis depth tunnel left: 19.5 meters;
- Vertical inter-axis: 7.5 meters;
- Horizontal inter-axis: 13.1 meters.

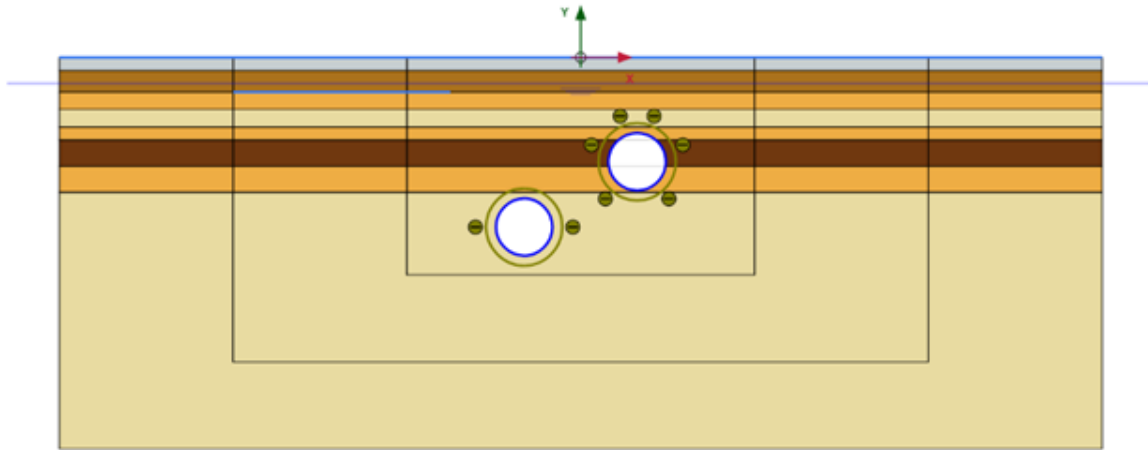


Figure 33 Offset configuration

Piggyback configuration (Figure 34):

- Axis depth upper tunnel: 12 meters;
- Axis depth bottom tunnel: 22 meters;
- Vertical inter-axis: 10 meters;

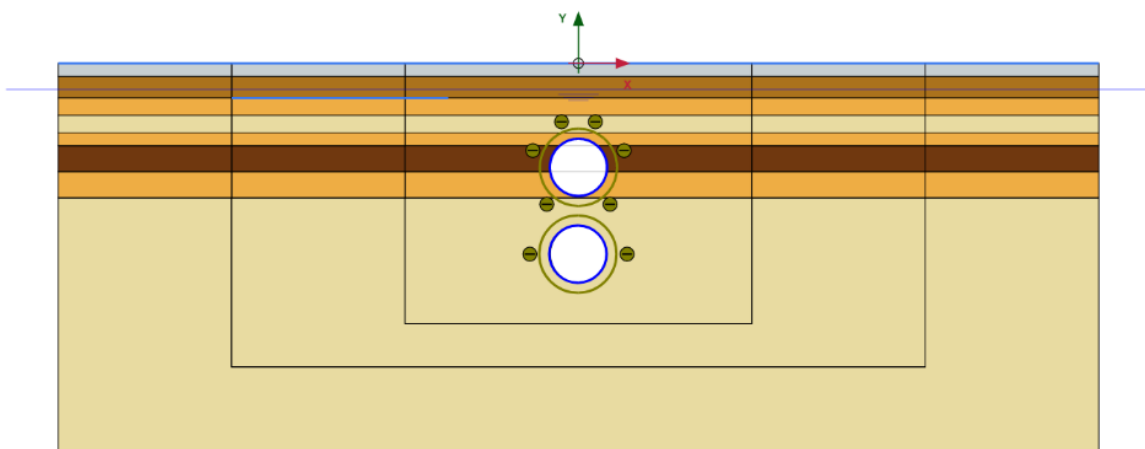


Figure 34 Piggyback configuration

After the definition of the geometry, it is necessary to generate the mesh. On PLAXIS 2D it is possible to set a very fine pattern for better results.

In order to not overweight the time calculations, the model is subdivided in three different zones: from far away from the tunnels up to reach the plate of the

lining, the mesh appears denser close the tunnels and coarser on the boundary, as shown in Figure 35.

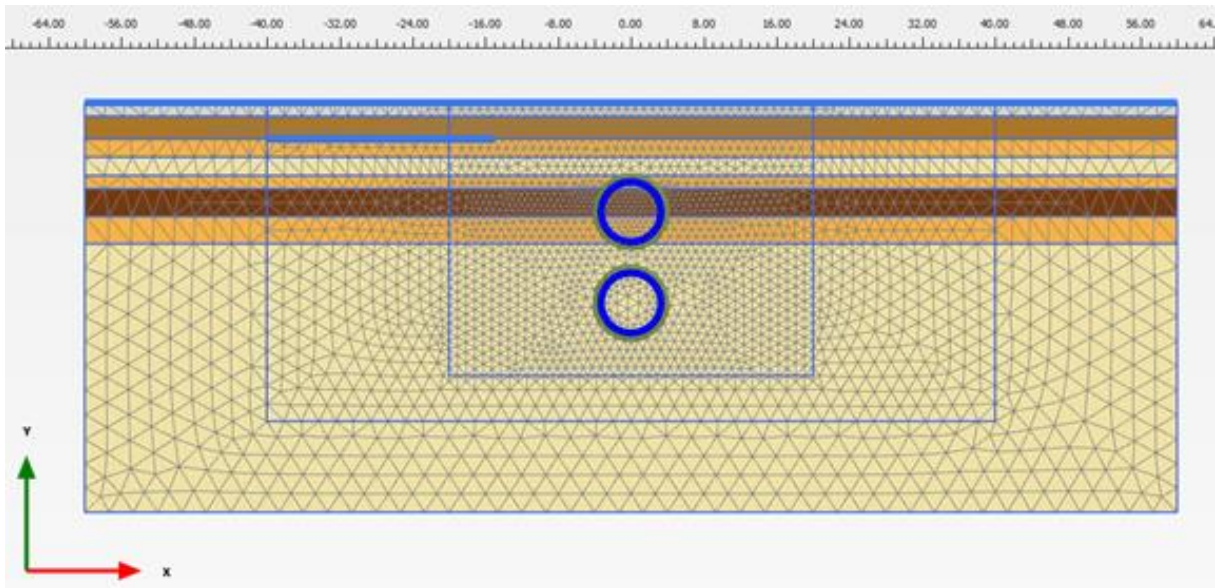


Figure 35 Mesh generation

5.2. Staged construction

Two different types of analysis are performed on PLAXIS 2D: the first regards the comparison among the three arrangements of the tunnels and the second goes in detail with the vertical layout. In PLAXIS the excavation simulation can be done in two different ways:

- Application of the deconfinement;
- Application of an internal radial pressure.

The construction stages are the same for each analysis, in particular:

1. Excavation of the first tunnel with the application of one of the two abovementioned methods;
2. Installation of the lining;
3. Excavation of the second tunnel as before.

5.2.1. Construction Stages with the three different alignments

The analysis of the three alignments is performed with the application of the deconfinement on the excavated zone. The idea is to simulate the progressive advancement of the machine towards the studied section by the application of a coefficient (β) to the initial stress before the tunnel is constructed.

$$p_f = (1 - \beta) * \sigma_0$$

This coefficient of deconfinement is introduced by (Panet, et al., 1974).

In practice, when the soil cluster is deactivated, this deconfinement value is applied in order to simulate the reduction of the initial stress due to the creation of the void. When the studied section is equal to the face-front, typical value of the deconfinement is about 28%. It means that only the 72% of the initial stress field acts as support around the tunnel. In the subsequent phases, the pressure has to be reduced up to the section in which the lining is installed. At this point, the deconfinement is maximum (100%), which means that the support pressure does not act anymore, and all the loads are transferred to the lining.

In order to select which is the value to insert in the deconfinement, a preliminary analysis is performed by imposing a percentage of volume loss on the surface; in this thesis the two volumes losses are equal to 0.5% and 1%. The volume loss is correlated to the deconfinement in the void: if the wanted volume loss is lower, the deconfinement will be lower and, consequently, the applied pressure p_f higher.

5.2.2. Construction Stages with vertical alignment

This analysis is carried out by simulating the excavation process thanks to the application of an internal radial pressure. This pressure varies increasing the

depth, taking into account the presence of the conditioned soil, which has a unit weight equal to 14 kN/m³.

Four different values are selected in order to conduct a parametric analysis: these values are chosen between the minimum support pressure required to stabilize the excavation and the maximum applicable one, as mentioned in the Chapter 4.4. The pressures values used in the analysis are listed in Table 10 below:

Table 10 Support pressures for twin tunnels

PRESSURE UPPER TUNNEL [kPa]	PRESSURE BOTTOM TUNNEL [kPa]
100	225
115	265
135	300
150	325

The parametric analysis is designed by fixing the pressure of the tunnel constructed first and varying the pressures related to the other one. In this way, it is possible to obtain sixteen pressure combination for each excavation sequence.

In the Figure 36, there is an example of this type of analysis. In particular, the upper tunnel is excavated with 1 bar (*1_P1*), then the lining is installed (*1_P1_Lining*), and the last four steps are related to the excavation of the bottom tunnel, varying the bottom pressure from 2.25 bar up to 3.25 bar (e.g. *1_P1-2.25_P2*). After that the pressure of excavation of the upper tunnel is fixed to 1.15 bar (*1.15_P1*) and again the bottom is excavated with the four pressures.

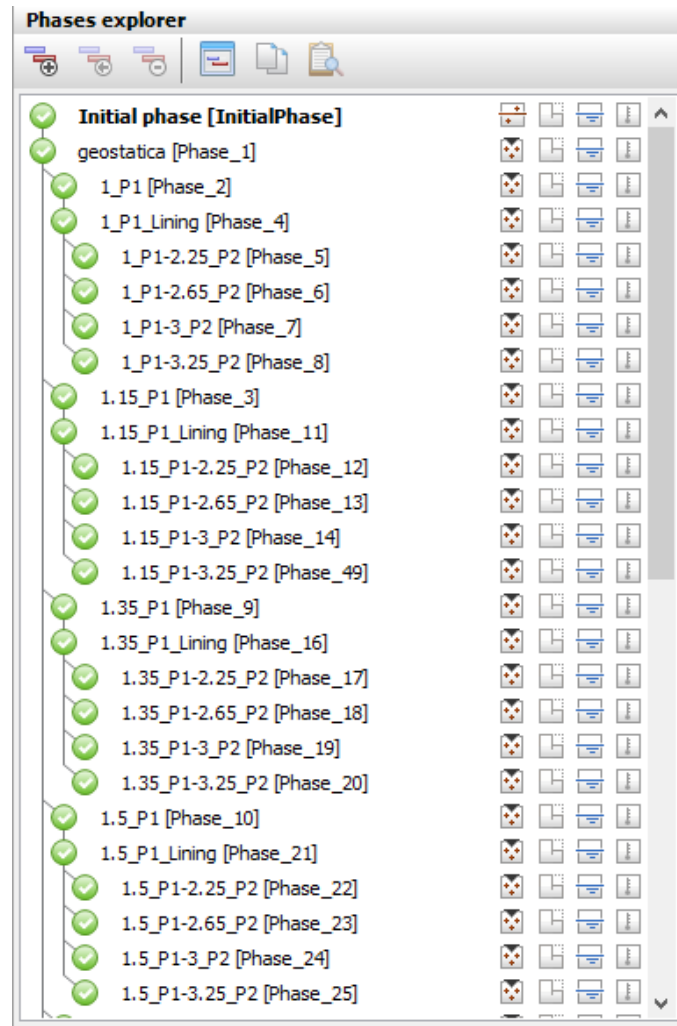


Figure 36 Stage Construction

All this procedure is repeated when the bottom tunnel is constructed first, starting with the application of 2.25 bar and varying the upper from one bar to 1.5 bar.

6. RESULTS AND INTERPRETATIONS

In this chapter, the results of all the different analysis are presented. At the beginning, the outputs of the 3D numerical FEM analysis changing the construction sequence are reported. Then, the results of the two 2D numerical FEM analysis are discussed:

- The worst arrangement analysis from the point of view of volume loss and maximum vertical settlement on ground surface;
- The parametric analysis changing the pressure combination with the aim to discover which is the worst construction sequence for piggyback tunnels under the point of view of induced settlements, volume loss and building damage.

6.1. Three-dimensional numerical analysis

The aim of the analysis is to define the worst construction sequence in terms of vertical settlement on the surface. After having set up the two construction processes, the upper tunnel excavated as first (U->B) and the bottom one excavated as first (B->U) (Chapter 4), the program Midas FEA NX automatically gives the outputs.

The displacement can be upwards, so their sign is positive, or downwards, hence the sign is negative. However, since the model is placed below the coordinate z equal to zero, the displacements will be all negative.

The results are displayed thanks to an automatic colour scale, which goes from the red colour that represents the smallest value to the blue one, which identifies the greatest value.

The outputs reporting vertical displacements (T_z) for both the construction sequences are shown in the Figure 37 and Figure 38 below.

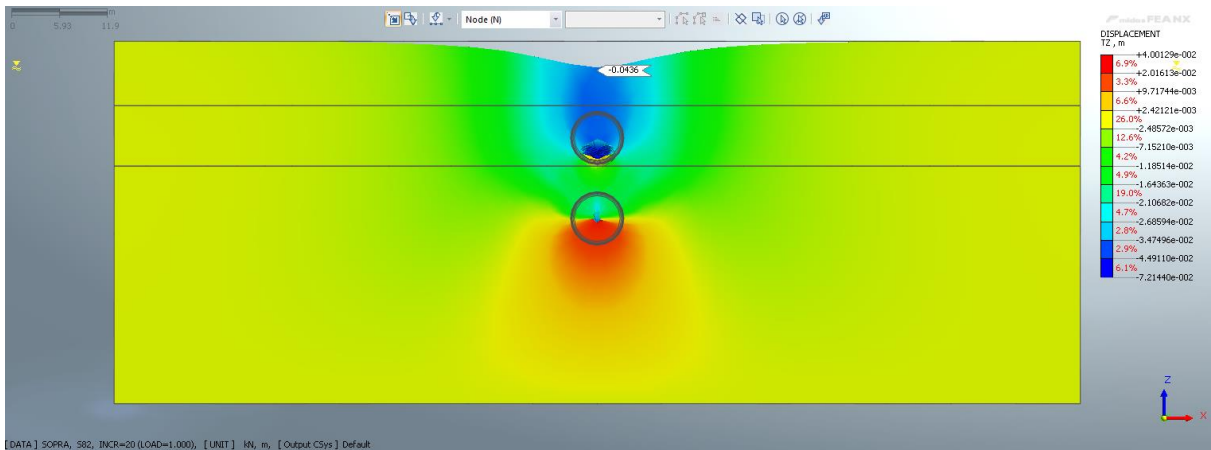


Figure 37 Vertical displacements upper first construction sequence

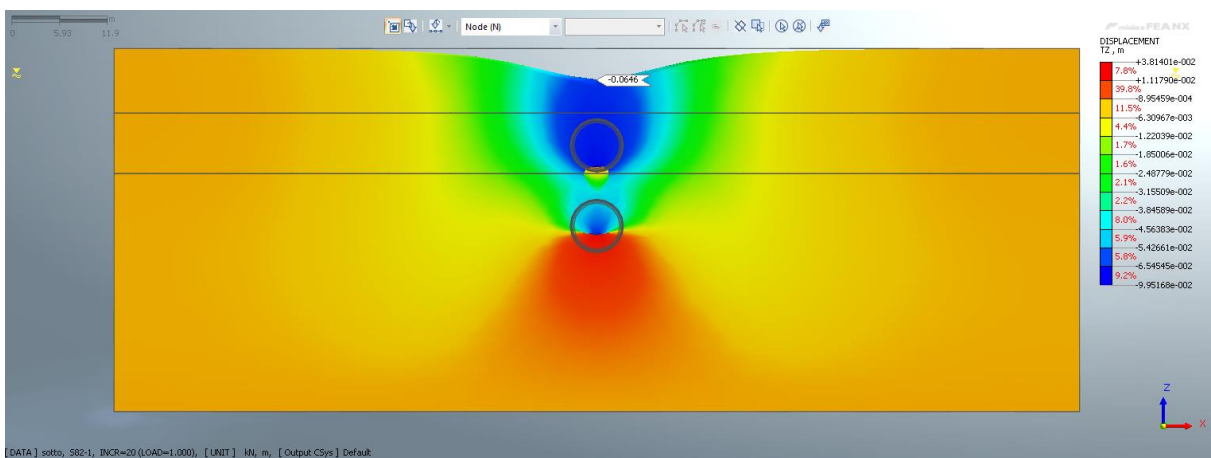


Figure 38 Vertical displacements bottom first construction sequence

It is possible to appreciate that the maximum vertical displacement recorded at the surface level is 4.4 cm for the U->B excavation sequence and 6.5 cm for the B->U one (Figure 39).

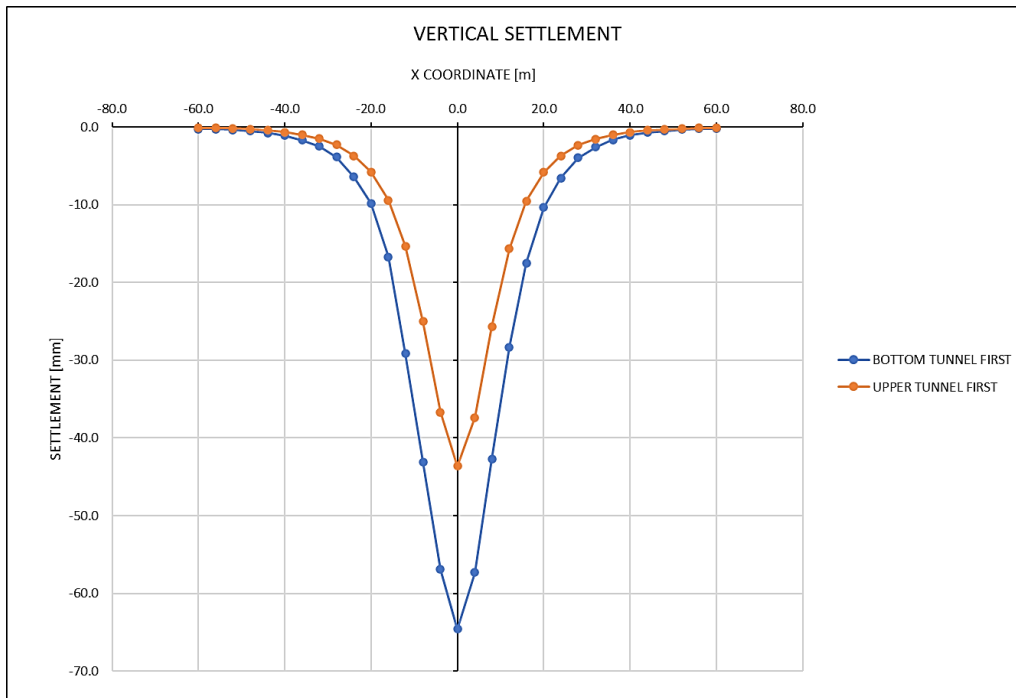


Figure 39 Comparison of the construction sequences: vertical settlement

At this point, it is possible to state that the construction sequence upper first U->B induces lower settlements than the other one because, when the bottom tunnel starts to be excavated, the lining of the upper one absorbs part of displacements locally improving the soil quality.

At the end, it is necessary to specify that the three-dimensional numerical analysis requires a lot of time for the definition of all the steps to reach an accurate result. For this reason, the other analysis will be performed with the software PLAXIS 2D, with which it is possible to carry out different types of investigation spending less time due to its simplicity in order to cross-check the general results and tunnel behaviour. However, the 3D modelling is the most powerful tool to represent the reality of the problems.

6.2. Two-dimensional analysis: worst arrangement

The aim of this two-dimensional modelling activity is to discover which are the worst arrangement of the twin tunnel and its worst excavation sequence. The examined layouts of the twin tunnels, as in the Figure 40, are:

- Horizontal;
- Offset;
- Vertical or piggyback.

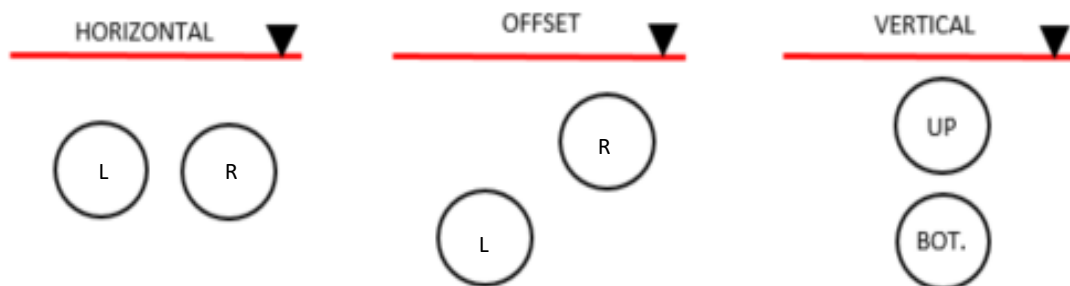


Figure 40 Layouts of the twin tunnels

The control parameters useful for the analysis are the maximum vertical surface settlement and the volume loss, both induced after the excavation of the second tunnel.

This study is conducting by simulating the advancement of the EPB machine thanks to the deconfinement method, already explained in the Chapter 5.

In order to correctly compare the different layouts, it is necessary to homogenise the volume losses induced by the excavation of the single tunnels. In particular, the work is conducted fixing two possible volume losses (VL_{single}) related to the single excavation:

- $VL_{\text{single}} = 0.5\%$
- $VL_{\text{single}} = 1.0\%$

Some preliminary analyses are required to retrieve the right value of the deconfinement related to the single tunnel to obtain these volume losses. The Table 11 reports the deconfinement values for the different positions of the tunnels following the denomination proposed in the Figure 40:

Table 11 Deconfinement values for single tunnels

CONFIGURATIONS	$VL_{\text{single}} = 0.5\%$	$VL_{\text{single}} = 1.0\%$
	DECONFINEMENT [%]	DECONFINEMENT [%]
HORIZONTAL	15	25
OFFSET R	15	26
OFFSET L	17	28
VERTICAL UP	15	26
VERTICAL BOTTOM	16	28

Once the deconfinements for the single tunnels are deducted, the analysis can start. Five numerical analyses are performed for each volume loss:

1. Horizontal arrangement;
2. Offset arrangement and the right tunnel is excavated as first;
3. Offset arrangement and the left tunnel is excavated as first;
4. Vertical arrangement and the upper tunnel is excavated as first;
5. Vertical arrangement and the bottom tunnel is excavated as first.

The results of these analysis are collected and then plotted in two graphs as the Figure 41 and the Figure 42 show. The graphs figure out the five subsidence troughs, hence, on the x-axis there is the x coordinate of the model, while on the y-axis the vertical settlement expressed in millimetres is represented.

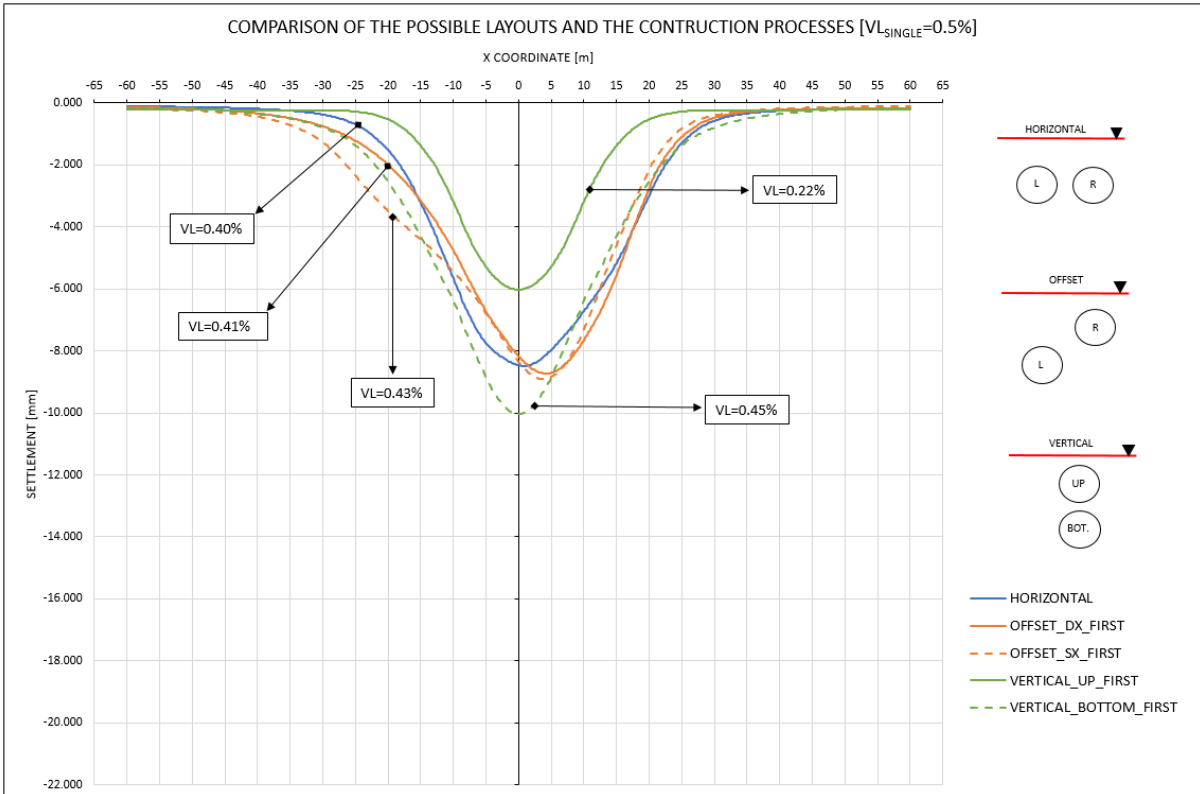


Figure 41 Results worst arrangement VL=0.5%

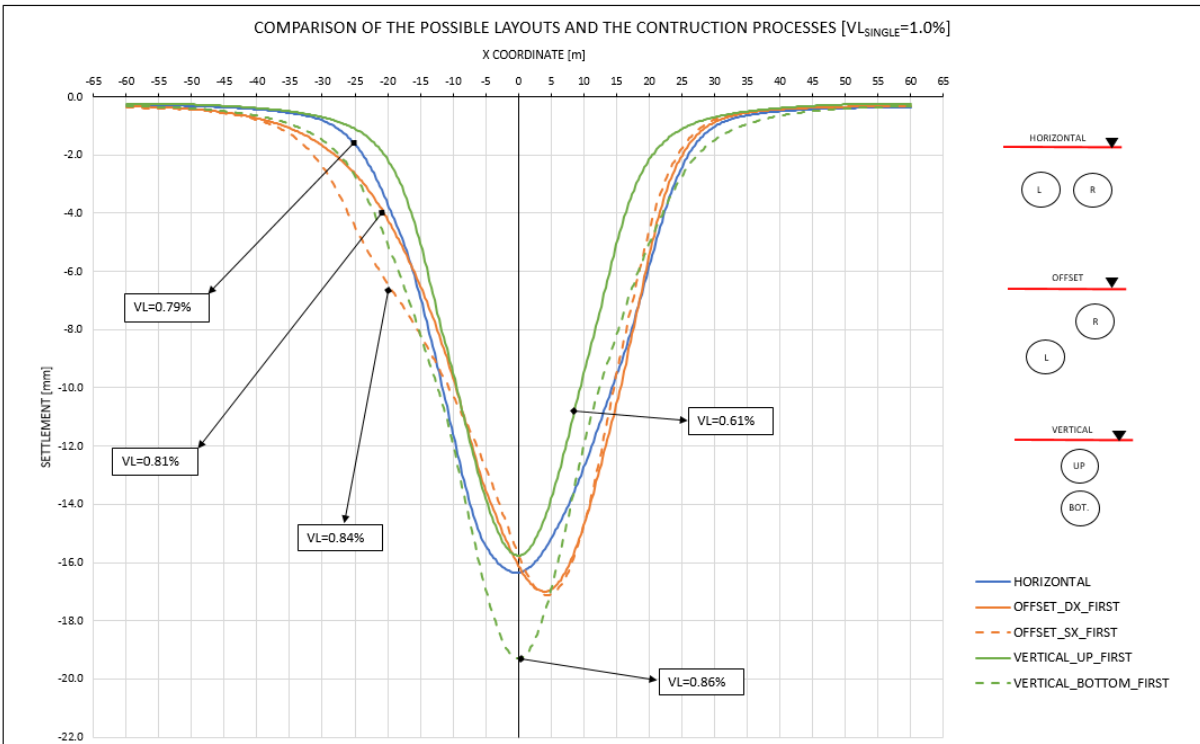


Figure 42 Results worst arrangement VL=1.0%

In conclusion, it is possible to state that the worst arrangement from the point of view of the vertical settlement and the volume loss is the vertical or piggyback layout when the bottom tunnel is constructed first. On the other hand, the best configuration is always the piggyback, but when the upper tunnel goes as first. This is explainable thanks to the fact that when the upper tunnel is excavated and the lining is installed, at the passage of the second tunnel, the lining produces a damping effect on the induced settlement of the bottom tunnel. This phenomenon does not occur or occurs in a less amount in the other configurations. Particularly for the worst arrangement, the settlement related to the single excavations are perfectly summed. The Figure 43 and Figure 44 highlight an example of the outputs on PLAXIS 2D related to the best configuration at the surface level and on the entire model.

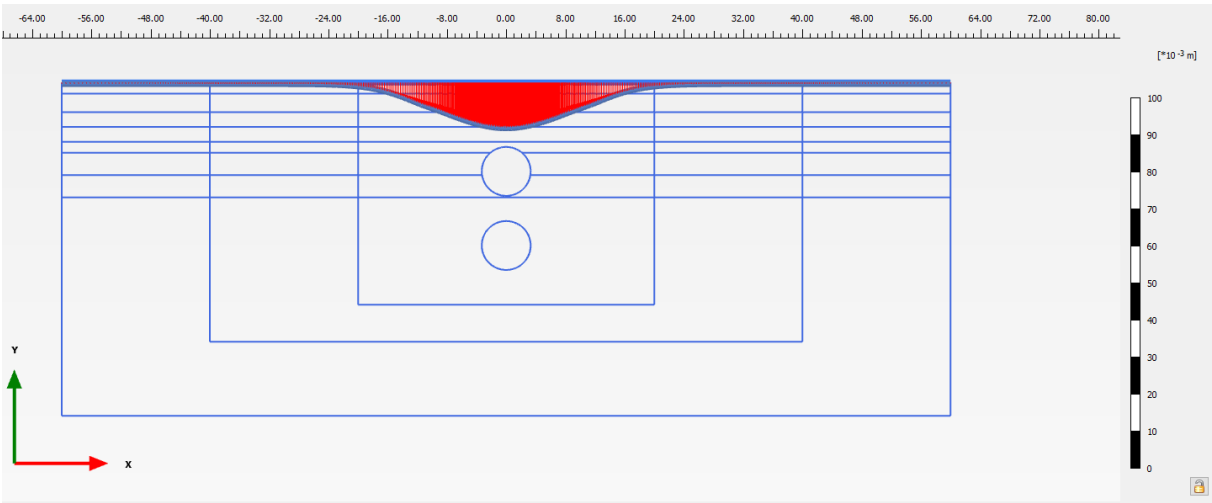


Figure 43 Piggyback upper first: surface displacements

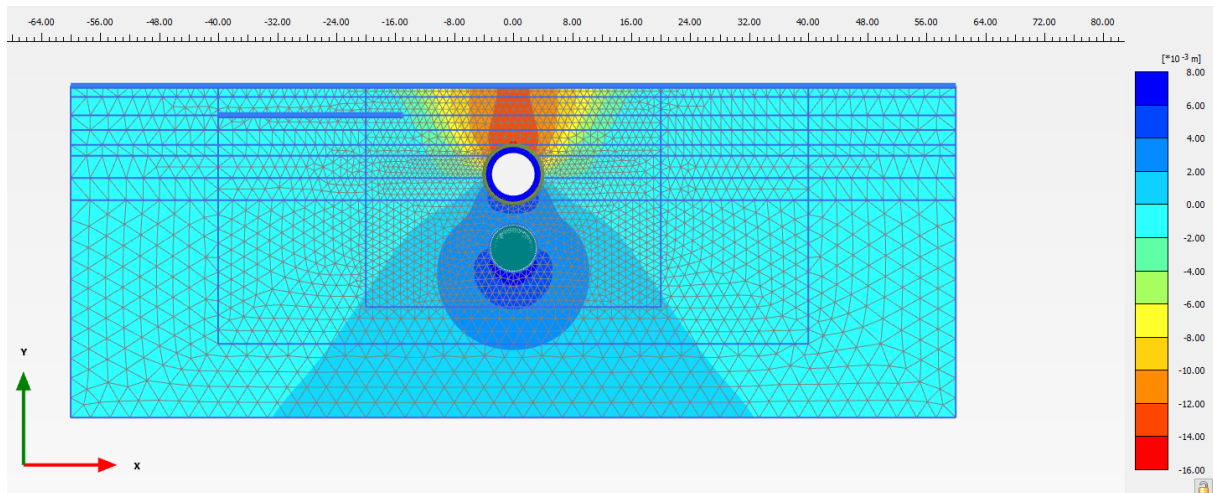


Figure 44 Piggyback upper first: vertical displacements

6.3. Two-dimensional analysis: piggyback tunnels

After having discovered that the worst configuration is the piggyback one, a series of analysis are conducted to look for the best pressure combination for the excavation of the twin tunnels and under the point of view of the induced damage on the buildings. To do that, two plates are designed in the model to collect the results, as shown with blue lines in Figure 45: one on the ground surface and the other at a depth of four meter from the surface (the depth of the foundation level). The latter plate is smaller than the ground surface one because its extent represents only the length of the studied building.

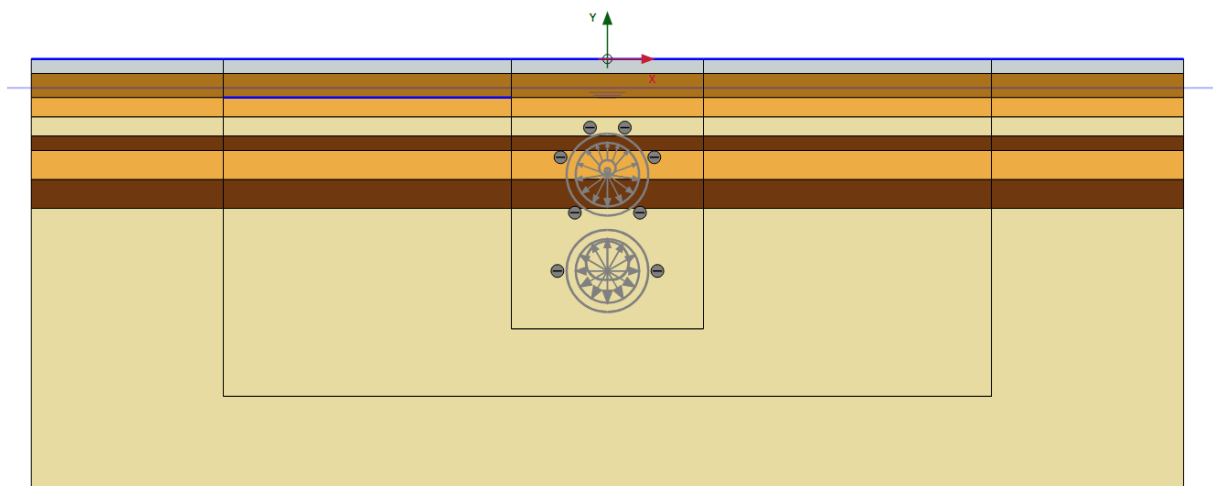


Figure 45 Plaxis 2D model for piggyback layout

This modelling activity is conducted, as previously said in the Chapter 5, by simulating the advancement of the EPB machine thanks to a radial and internal support pressure for both the tunnels. Once the machine is advanced and the lining must be installed, this pressure is turned off. The pressure values used in the tests are listed in the below:

The pressures for the upper tunnel are:

- 1.0 bar;
- 1.15 bar;
- 1.35 bar;
- 1.5 bar.

The pressures for the bottom tunnel are:

- 2.25 bar;
- 2.65 bar;
- 3.0 bar;
- 3.25 bar.

6.3.1. Best construction sequence and pressure combination

A preliminary analysis is needed to check how the various pressure combinations affect the two excavation sequences. For these reason four control parameters are selected:

- The volume loss (VL);
- The maximum vertical settlement (U_{max});
- The maximum angular distortion (β_{max});
- The position of the inflection point (i).

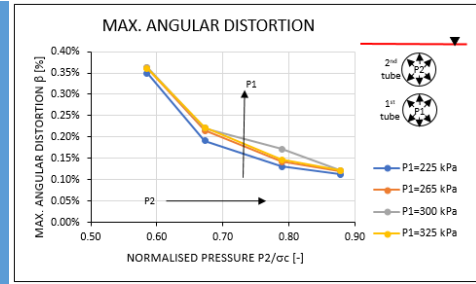
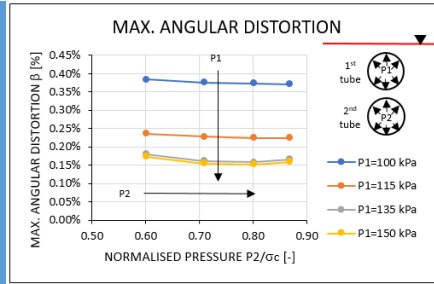
This test is performed by fixing the pressure of the tunnel excavated first (P1) and varying the pressure of the other one (P2). The outputs of this test campaign

are reported in the Table 12 below normalizing the support pressure P2 with the geostatic one σ_c .

Table 12 Outputs for the two different construction sequence

		UPPER TUNNEL EXCAVATED AS FIRST	BOTTOM TUNNEL EXCAVATED AS FIRST
VOLUME LOSS	VOLUME LOSS		
		The volume loss reduces either increasing the pressure P1 or fixing the P1 and increasing only P2.	
MAXIMUM VERTICAL DISPLACEMENT	DISPLACEMENT		
		The maximum vertical displacement reduces either increasing the pressure P1 or fixing the P1 and increasing only P2.	

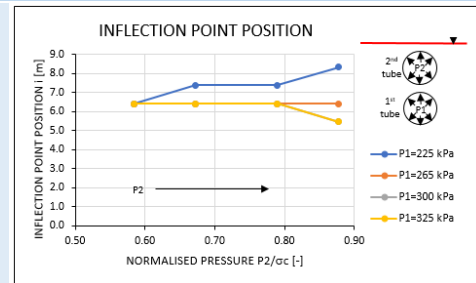
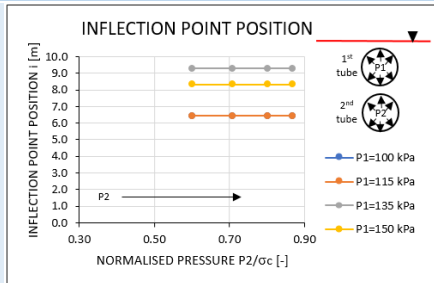
MAXIMUM ANGULAR DISTORTION



Increasing the pressure P1 the maximum angular distortion reduces, while by fixing the P1 and increasing only P2 almost no changes are reported

Increasing the pressure P1 the maximum angular distortion increases too, while by fixing the P1 and increasing only P2 a reduction of β_{max} occurs.

INFLECTION POINT POSITION



The inflection point position does not show a defined trend

Once all the results for both the tunnel are plotted and analysed, a comparison must be done. Obviously, the inflection point outputs are discarded because it is not possible to define a precise behaviour.

In order to make the two cases comparable, a mean normalised pressure is computed and a filtering operation on the couples of results, which have almost the same normalised pressure, is carried out. This activity led to the construction of a trend line. The Figure 46, Figure 47 and Figure 48 display the comparison between the two examined construction sequences.

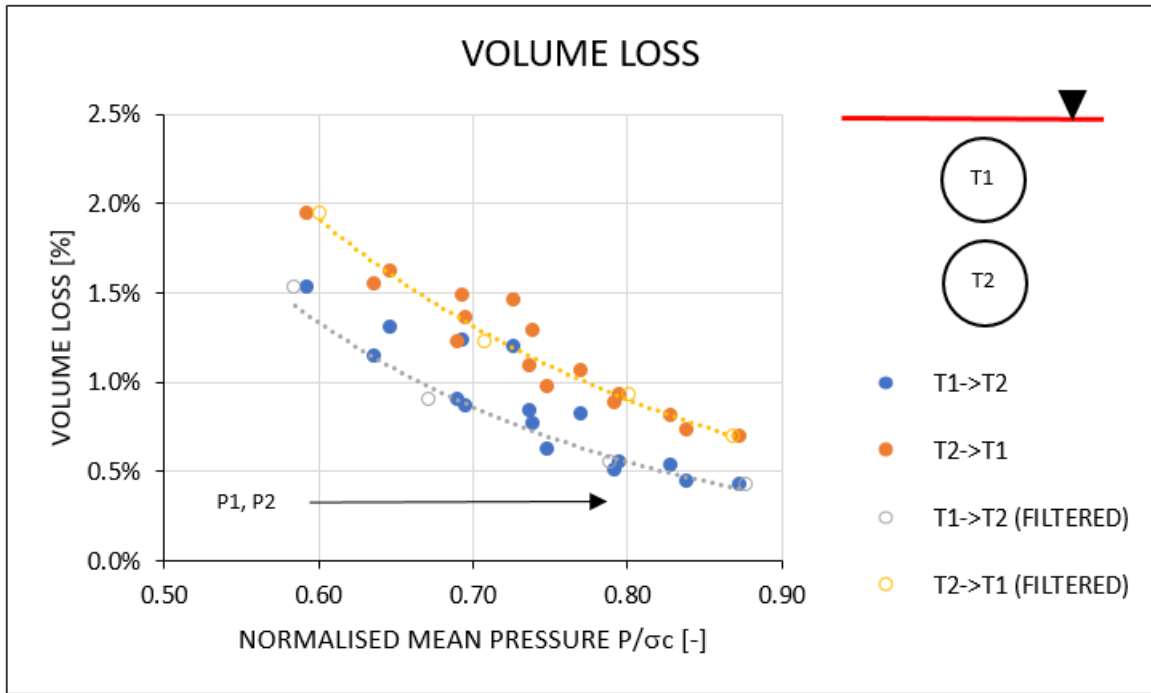


Figure 46 Comparison of the construction sequences: volume loss

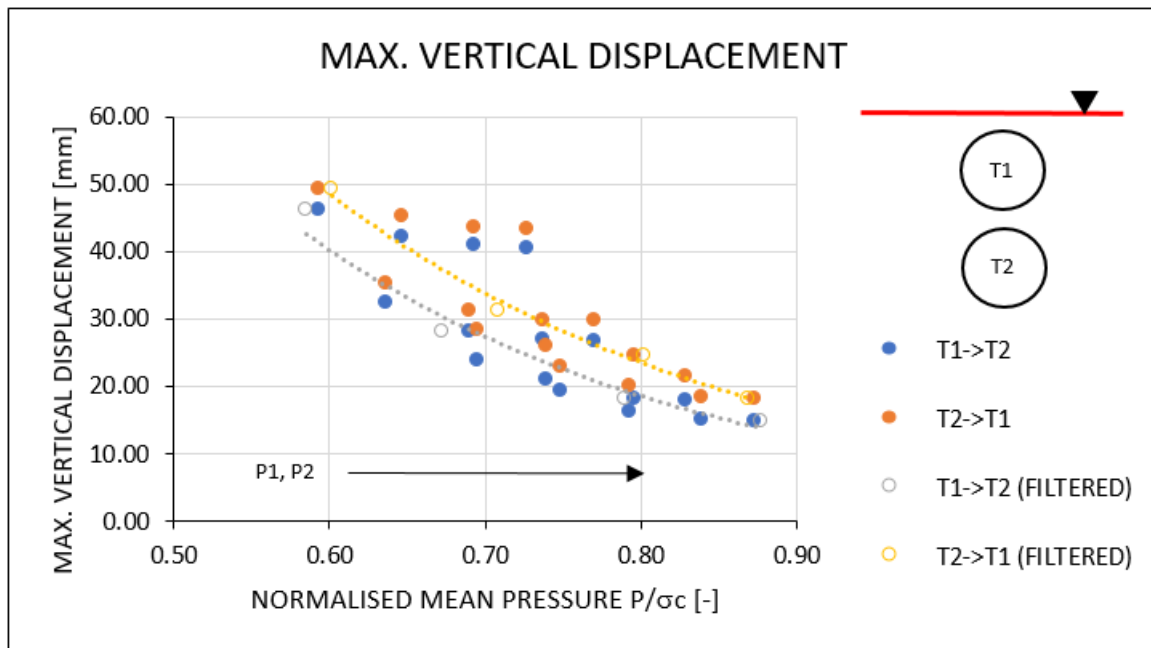


Figure 47 Comparison of the construction sequences: maximum vertical displacement

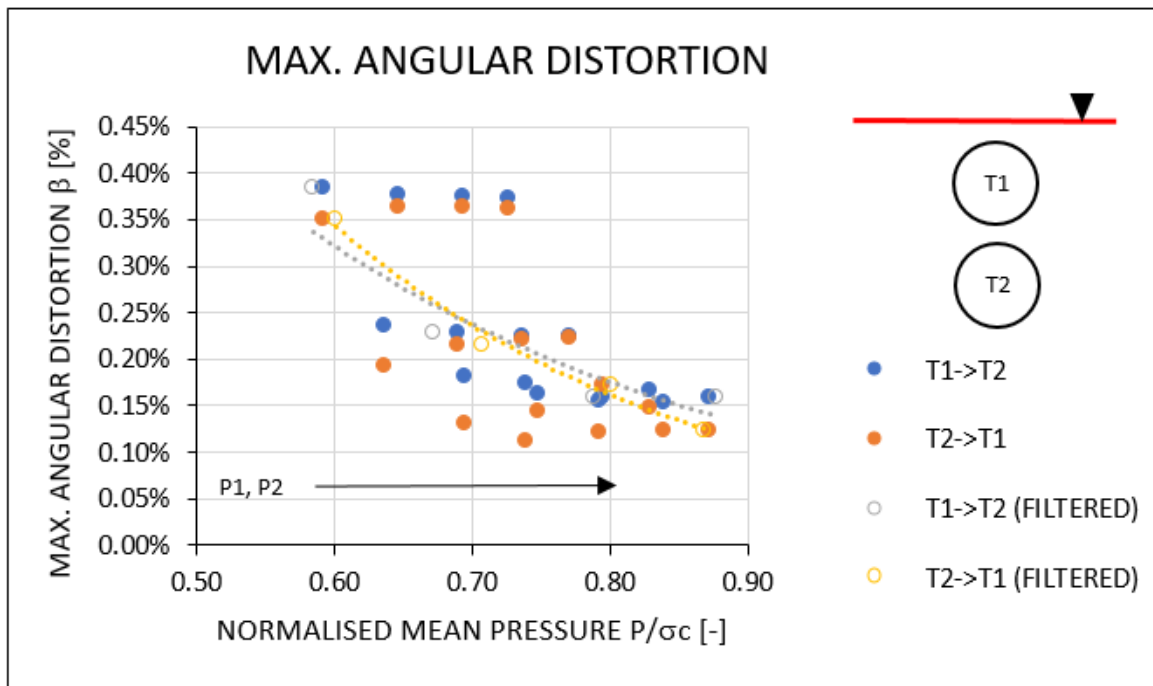


Figure 48 Comparison of the construction sequences: maximum angular distortion

As it is possible to appreciate, the volume loss and maximum vertical settlement are lower for the upper first construction sequence T1->T2. The smallest values are obtained for the pressure combination P1 equal to 150 kPa and P2 equal to 325 kPa. This couple of pressures induces a volume loss of about 0.42% and a maximum vertical displacement of about 14 mm. Moreover, about the maximum angular distortion, it is possible to state that the construction sequence does not affect it; it means that regardless of tunnels excavation order, the shape of the settlement trough remains the same. However, the only effect is given by the increase of the support pressure, which led to a reduction in the maximum value of β .

6.3.2. Induced damage on the buildings

The second step of this analysis is to conduct a Building Risk Assessment (BRA) on a selected structure and to obtain a risk category for each construction sequence and for each pressure combination.

The first phase is the identification of buildings located in the area interested by the tunnels excavation. It is imagined having a building placed at a distance of 10 m from the tunnel axis, as illustrated in Figure 49, and with the characteristics listed in the Table 13. A Building Condition Survey (BCS) is performed on the studied building: the vulnerability index (I_v) results equal to 90, which corresponds to a high vulnerability class, as shown in the Table 1.

Table 13 Building characteristics

PARAMETER	UNIT OF MEASURE	VALUE
Length (L)	[m]	30
Height (H)	[m]	20
Inertia moment (I)	[m ⁴ /m]	2267
Tangential and longitudinal elasticity modulus ratio (E/G)	[-]	2.6
Left vertex position (x_L)	[m]	-40
Right vertex position (x_R)	[m]	-10
Vulnerability index (I_v)	[-]	90

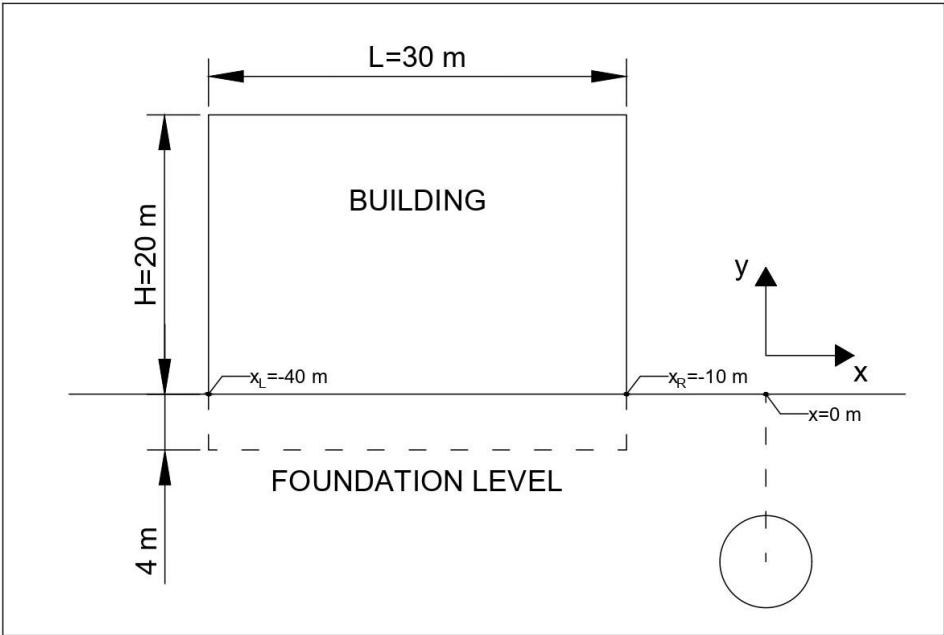


Figure 49 Position and geometrical characteristics of the building

Once the building parameters are defined and the data related to the vertical settlement are collected from the software, as an example reported in the Figure 50, the first aspect that is verified is the position of the building with respect to the settlement trough. The way in which the total deformations are computed changes if the building is placed in the sagging zone, in the hogging zone or in both of them (Figure 13).

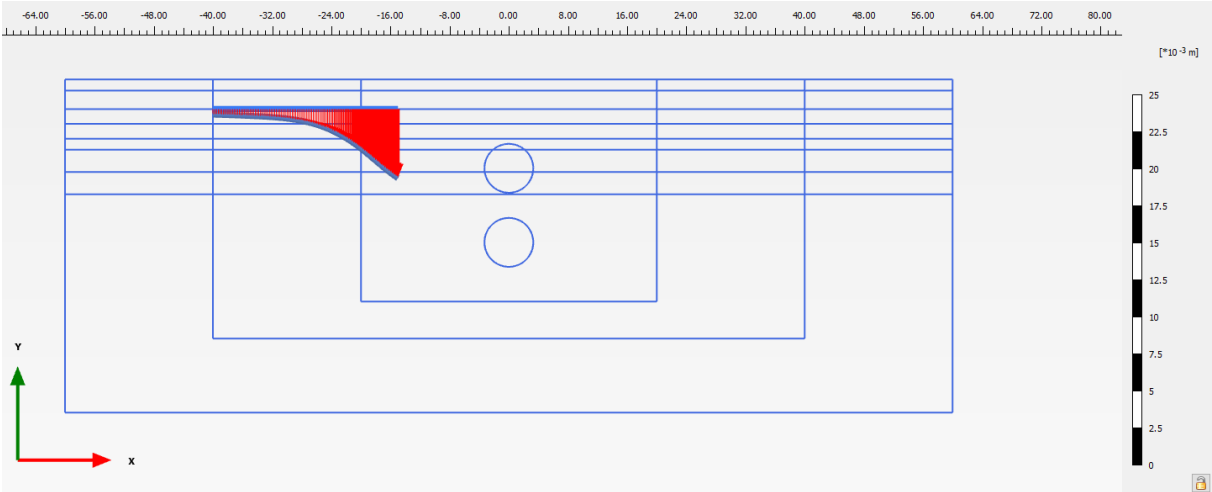


Figure 50 Building foundation settlement

This verification is conducted both for the settlement trough induced after the passage of the second tunnel and for the excavation the first one in order to also investigate the transient construction stage.

It is possible to state that the position of the inflection point at the surface level never reach the coordinate of the right vertex of the building, apart from the case of the single excavation of the bottom tunnel. It means that because of the theory that the inflection point approaches the position of the tunnel axis going deeper, as reported in the Figure 51, the building foundation falls always in the hogging zone. However, for the bottom tunnel construction, the building is divided in a portion in the hogging zone and another in the sagging one.

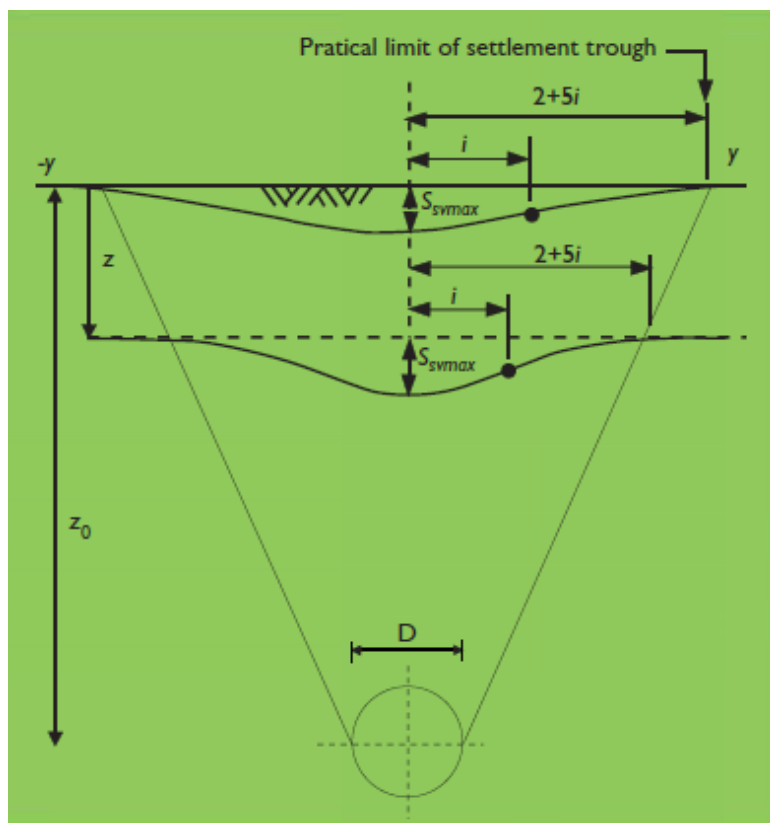


Figure 51 Subsurface settlement

The next step is to compute the control parameters, highlighted in the Chapter 3: the maximum vertical settlement (U_{\max}), the maximum angular distortion (β_{\max}) and the total deformation (ϵ_t). Then, it is possible to compare each of these parameters with the thresholds reported in the Table 4 and Table 5 to obtain the damage category. An example of this procedure performed for each pressure combination is reported in the Table 14 below.

Table 14 Example of damage class evaluation procedure

CONTROL PARAMETER	VALUE	LOWER THRESHOLD	UPPER THRESHOLD	DAMAGE CATEGORY	DAMAGE CLASS
ϵ_t [%]	0.0243	0	0.025	1	3
U_{\max} [mm]	15.17	5	25	2	
β_{\max} [-]	0.00295	0.0025	0.01	3	

The maximum category represents the damage class of the building. The Figure 52 and Figure 53 show the category of damage for each construction sequence and for every pressure combination.

As it is possible to appreciate almost a great part of the pressure combinations for both the construction sequences produce a damage category 2. Moreover, when the upper tunnel is excavated as first, the excavation of the second tunnel does not affect the damage category, but only the increase of the pressure of the upper tunnel induces a damage category reduction because of the damping effect of the installed lining. On the other hand, when the bottom tunnel is excavated as first, the increase of the excavation pressure of second tunnel plays a role in the reduction of the damage class.

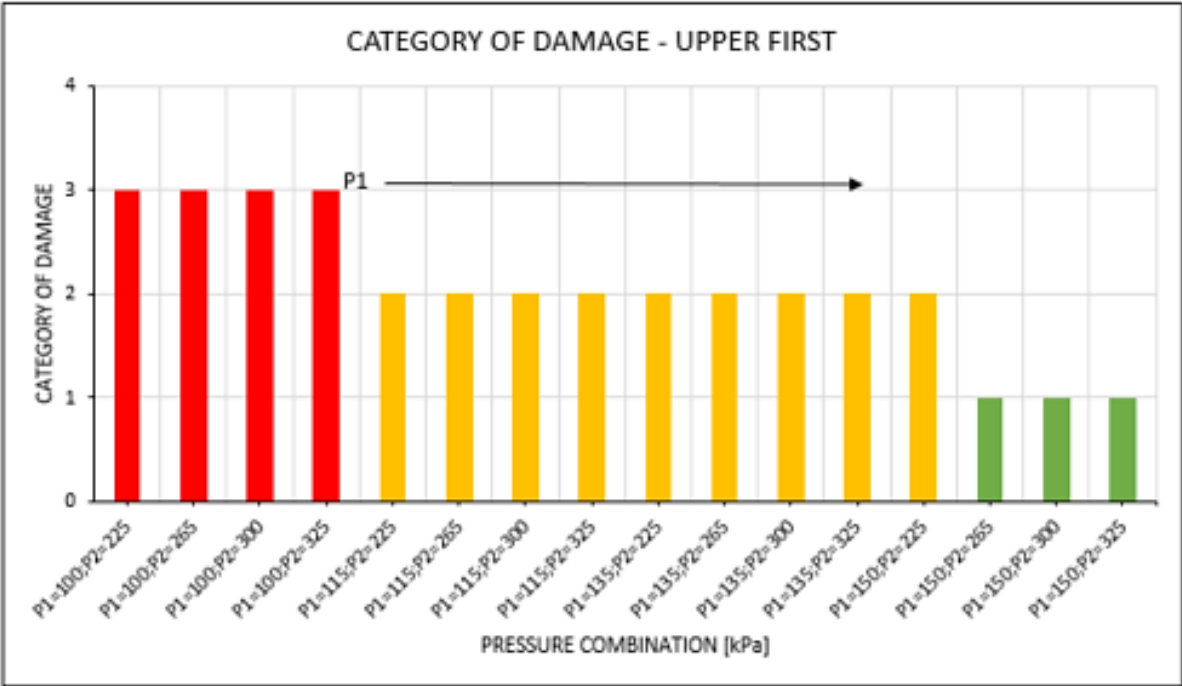


Figure 52 Category of damage - upper first

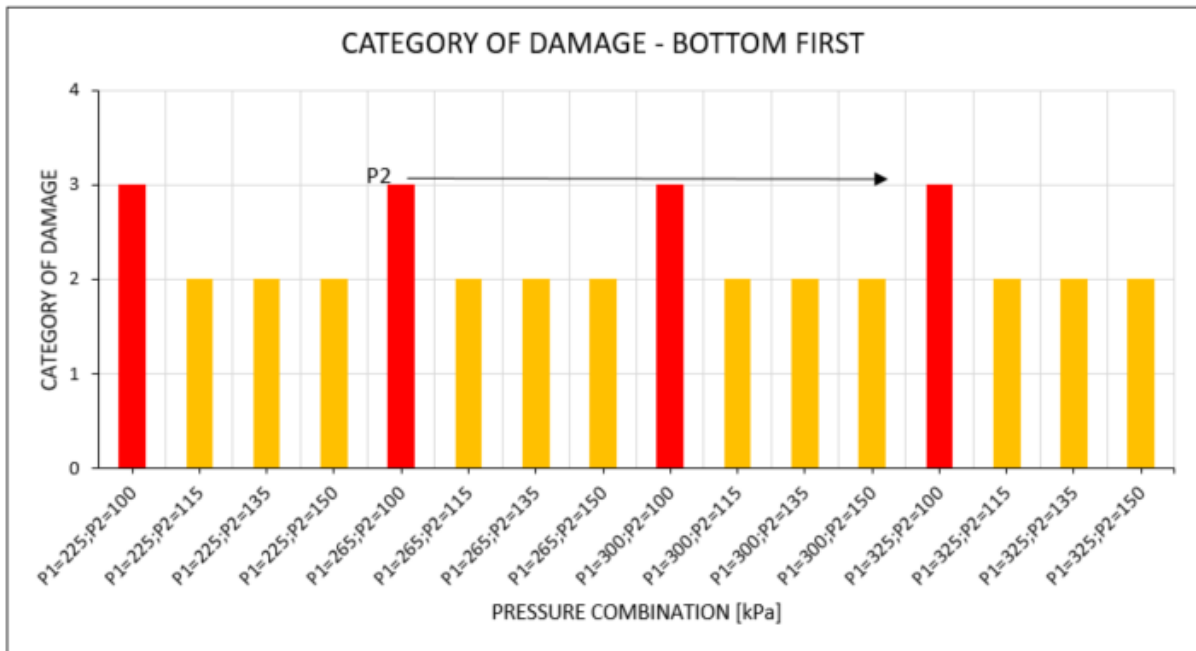


Figure 53 Category of damage - bottom first

Furthermore, a risk matrix can be defined by combining the vulnerability index and the category of damage, as displayed in the Figure 54 below. The risk can be:

- **Low (green):** no further actions are needed, but only standard monitoring system during the excavation of tunnels;
- **Medium (yellow):** 2D numerical models are probably needed and also a detailed monitoring system;
- **High (red):** 2D and 3D numerical models are required. In addition to the detailed monitoring system, the ground improvement treatments are designed based on the position of buildings respect to the tunnels.

Entering with the high vulnerability class and with the damage class of the building, the risk class can be Medium or High based on the pressure combination and the construction sequence.

Vulnerability class/ Damage class	Negligible	Low	Slight	Moderate	High
1	1	1	1	1	2
2	1	1	2	2	2
3	1	2	2	3	3
4	2	3	3	3	3

Figure 54 Risk matrix related to the studied project

The final step is to collect all the abovementioned information in three graphs related to the damage category parameters in order to perform a comparison. The Figure 55, Figure 56 and Figure 57 report how the maximum angular deformation in the upper tunnel as first construction sequence and the maximum vertical displacement in the other configuration dictate the category of damage for each pressure combination.

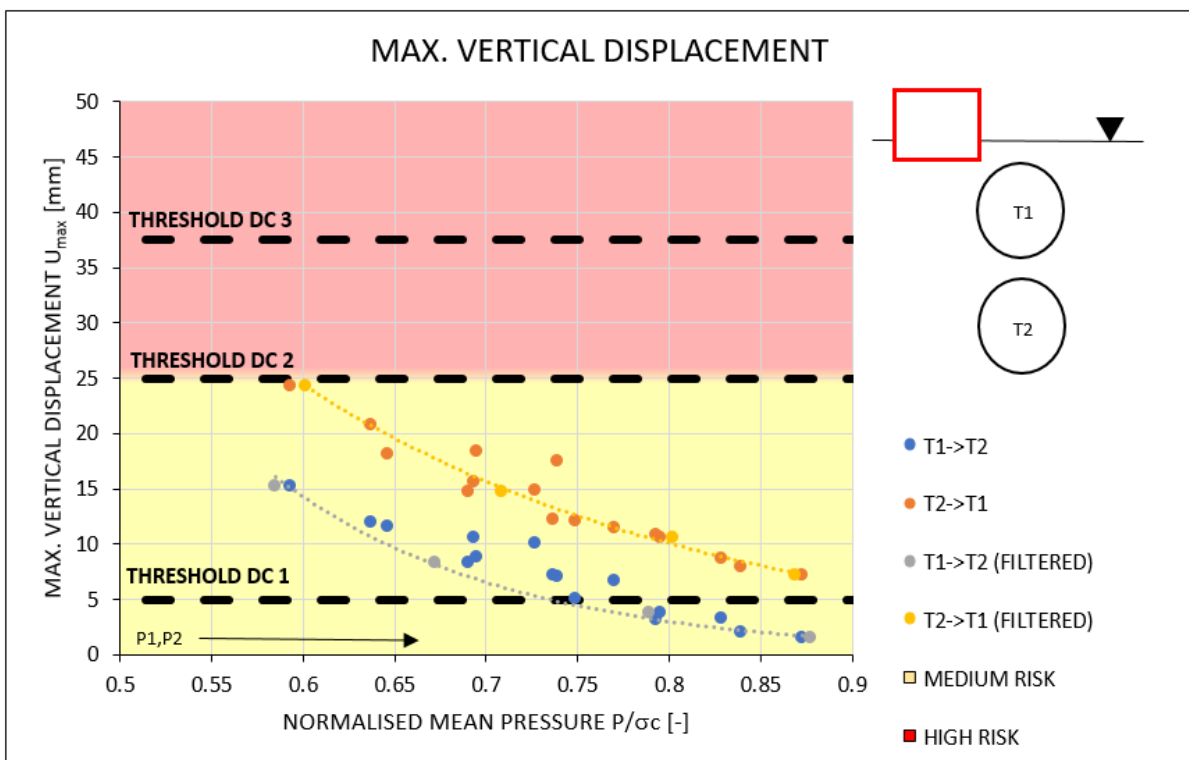


Figure 55 Risk related to the maximum vertical deformation

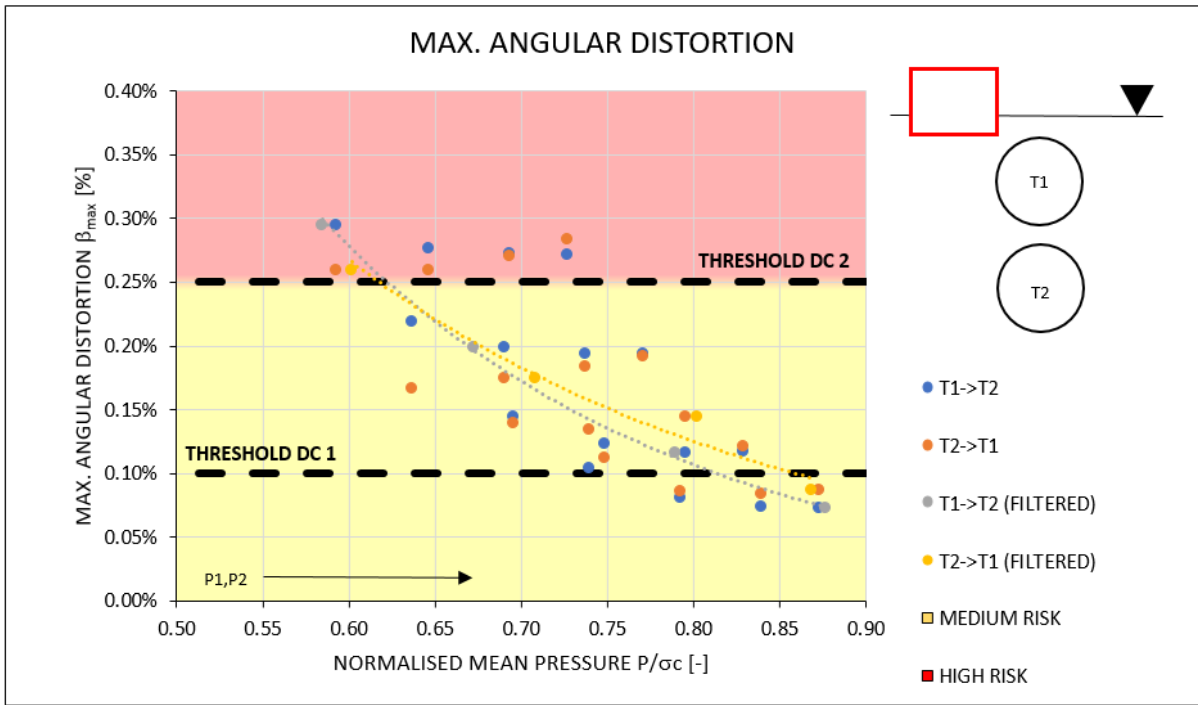


Figure 56 Risk related to the maximum angular distortion

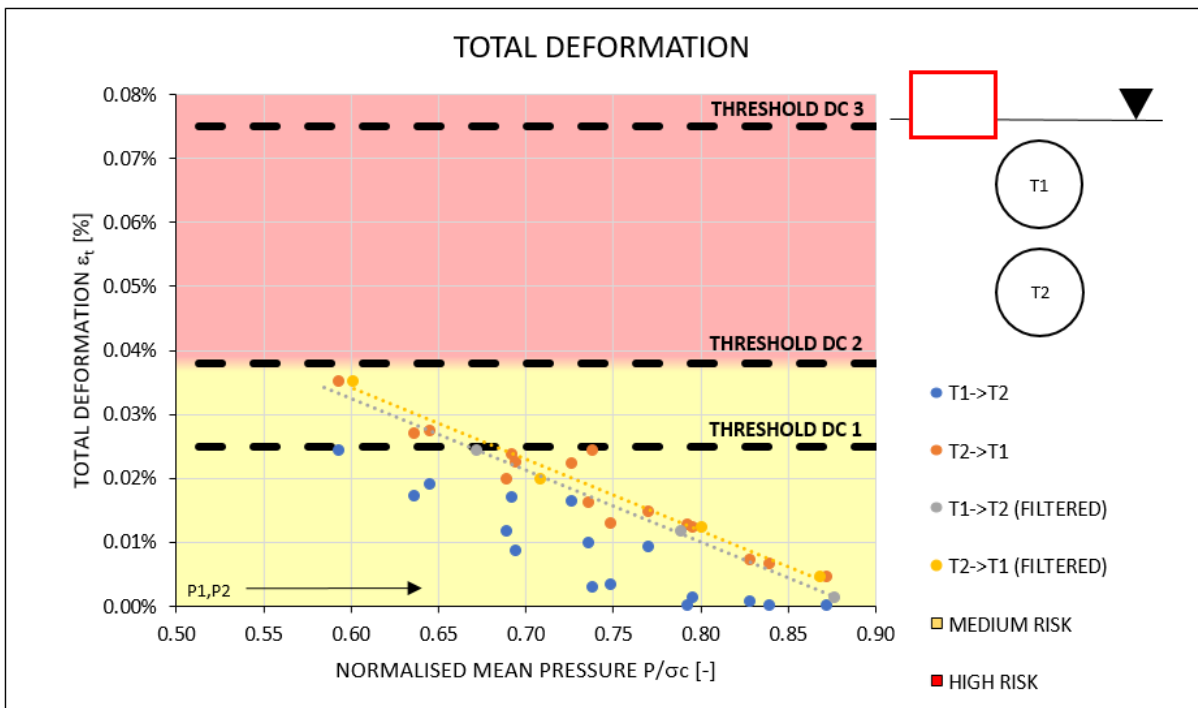


Figure 57 Risk related to the total deformation

Moreover, it is noticeable that almost all the pressure combinations for both the construction sequences fall in the risk class 2, eight in class 3 and three combinations give a risk class equal to 1.

At the end, it is possible to conclude that, under the point of view of the induced damage on the building, the best construction sequence is the upper excavated as first and the best pressure combinations are:

- $P1 = 150 \text{ kPa}$ and $P2 = 265 \text{ kPa}$;
- $P1 = 150 \text{ kPa}$ and $P2 = 300 \text{ kPa}$;
- $P1 = 150 \text{ kPa}$ and $P2 = 325 \text{ kPa}$.

7. CONCLUSIONS

The aim of this work is to analyse the excavation of twin tunnels in urban area under the point of view of the induced settlements and of the damage triggered on the buildings changing the construction sequence thanks to the numerical modelling activity.

To do that the project of M5 metro line in Bucharest, designed by the company Systra SWS, is taken as reference. This project is characterised by 22 stations and 2 tunnels, which change their relative position along the pathway that runs from Drumul-Taberei district to Pantelimon area. The tunnels are excavated with the Earth Pressure Balance (EPB) machine able to create the void and install the lining at the same time.

The study is developed using the three-dimensional FEM numerical software Midas FEA NX and the two-dimensional FEM numerical software PLAXIS 2D. In the models, the stratigraphy is obtained by the already preformed borehole surveys, which allow the definition of seven geological units. In addition, for the soil, a Hardening Soil constitutive model is selected, while for the structural elements a Linear Elastic constitutive model is more suitable. The piggyback tunnels arrangement is selected for the 3D numerical analysis due to its peculiarity with the aim to compare the two construction sequences based on vertical displacements. On the other hand, a study for the three possible layouts (horizontal, offset and piggyback) and then a focus on the vertical configuration are investigated with a 2D modelling activity. The scope is to evaluate which is the worst (under the point of view of induced settlements) twin tunnels arrangement varying the construction sequences and the best (based on the induced building damage) piggyback excavation sequence varying the pressure combination.

In the 3D model, the excavation is simulated considering all the construction stages: the advancement of the machine, the application of the support pressure at the face front, the passage of the shield, the lining installation and the grout injection to fill the annular gap.

Looking at the 2D models, the advancement of the machine is simulated thanks to two methods: the deconfinement and the internal radial support pressure. In particular, the first one is applied for the worst layout analysis and the second one for the building induced damage investigation.

The results of the numerical analyses highlight:

- For the piggyback arrangement, the construction of the upper tunnels as first leads to lower induced settlement than the sequence of the bottom tunnel excavated first. This phenomenon is caused by the damping effect due to the presence of the upper lining, which absorbs part of the displacements triggered by the bottom tunnel excavation that never reach the ground surface and stiffens the soil. Furthermore, when the bottom tunnel is excavated first, a de-tensioning of the surrounding soil up is induced. Therefore, the subsequent excavation of the tunnel above within this de-tensioned soil (mostly yielded) implies further deformations and settlements with a considerable increasing of settlements. This behaviour is manifested in both 3D and 2D numerical models;
- About the worst tunnels arrangement, the study demonstrates that the piggyback configuration represents both the best and the worst case in term of settlements and volume loss. In fact, the upper first sequence induces the smallest values of them, while the bottom first sequence shows the maximum vertical settlement and volume loss for the abovementioned reasons. Ranking all the configuration and their construction processes from the best to the worst one: piggyback upper

first, horizontal, offset right first, offset left first and piggyback bottom first. Furthermore, the damping effect of the lining installation explains the lower settlement and volume loss recorded for the right first offset layout with respect to the left first;

- Under the point of view of the induced damage on the buildings caused by the piggyback twin tunnels excavation, the damage category is the lowest excavating the upper tunnel as first and increasing the support pressures combination. In fact, the increase of the excavation pressure, approaching the geostatic stress field, induces lower displacements because the “ground feels less the excavation”. However, the lowest risk class is always Medium for both the construction sequences hence, under the point of risk, it is not possible to identify the best sequence.

ACKNOWLEDGEMENTS

I want to thank prof. Daniele Peila, who follows me in this work giving me the possibility to improve my knowing and myself.

Moreover, I want to express my gratitude to Systra SWS Company, especially to Eng. Michele Palomba and his team with whom I lived this adventure, called thesis, helping me with their infinite availability and kindness showed in every moment.

BIBLIOGRAPHY

Anagnostou G e Kovari K Face stability condition with Earth Pressure Balanced Shields. - 1996.

Attewell P B e Woodman J P Predicting the dynamics of ground settlement and its derivatives caused by tunnelling in soil // Ground Engineering. - 1982.

Attewell P B, Yeates Y e Selby A R Soil movements induced by tunnelling and their effects on pipelines and structures. - 1986.

Boscardin M Building response to excavation-induced ground movements. - 1980.

Boscardin M D e Cording E J Building response to excavation-induced settlement. - 1989.

Burland J e Wroth C Settlement of buildings and associated damage. - 1974.

Burland J P, Broms B B e De Mello V F B Behaviour of Foundation and structure. - 1977.

Chiriotti E, Marchioni V e Grasso P Interpretation of the results of the building condition survey and preliminary assessment of risk. Methodology for assessing the tunnelling induced risks on buildings along the tunnel alignment.. - 2000.

DAUB Reccomandations for face support pressure calculations for shield tunnelling in soft ground . - 2016.

DAUB Reccomendation for face support pressure calculations for shield tunnelling in soft ground . - 2016.

Do Ngoc-Anh, Dias D e Oreste P Three-dimensional numerical simulation of mechanised twin stacked tunnels in soft ground. - 2014.

Guglielmetti V [et al.] Mechanised tunnelling in urban area: design methodology and construction control. - 2007.

Hunt D Predicting the ground movements above twin tunnels constructed in London clay. - 2005.

Lee K M, Rowe R K and Lo K Y Subsidence owing to tunnelling. Estimating the gap parameter. - 1992. - pp. 929-940.

Loganathan N e Poulos H G Pile response caused by tunnelling. - 1998.

Mair R, J e Taylor R, N Bored tunnelling in the urban environment . - 1997.

Malvaso E 3D And 2D numerical models of mechanised excavation of overlapped tunnels in urban areas: sensitivity analysis of the stresses and the strain in the segmental tunnel lining varying the excavation sequence.. - 2022.

Martos F Concerning an approximate equation of the subsidence trough and its time factors. // Int. Strata Control Congress . - 1958.

MIDAS User Manual FEA NX. - 2021.

New B M e O'Reilly M P Tunnelling induced ground movements: predicting their magnitude and effects. - 1991.

O'Reilly M P e New B M Settlement above tunnels in the United Kingdom - their magnitude and prediction. - 1982. - p. 173-181.

Panet M e Guellec P Contribution à l'étude du soutènement d'un tunnel à l'arrière du front de taille. - 1974.

Panet M. e P. Guellec Contribution à L'étude du soutènement d'un tunnel à l'arrière du front de taille. . - 1974.

Peck R B Deep excavations and tunnelling in soft ground. - 1969. - p. 225-290.

R J, Mair e R N Taylor Bored tunnelling in the urban environment . - 1997.

Rankin W J Ground movements resulting from urban tunnelling: prediction and effects. - 1988.

Schmidt B Settlement and ground movements associated with tunnelling in soil . - 1969.

Shah R [et al.] Influencing factors affecting the numerical simulation of the mechanized tunnel excavation using FEM and FDM techniques [Journal]. - 2017.

Skempton AW e MacDonald D H The allowable settlements of buildings. - 1956.

Verruijt A e Booker J R Surface settlements due to deformation of a tunnel in an elastic half plane. - 1996. - Vol. 46.

FIGURE INDEX

Figure 1 Existing underground network	3
Figure 2 M5 metro line.....	5
Figure 3 Stratigraphy of the project area.....	7
Figure 4 Earth Pressure Balance machine (EPB)	8
Figure 5 Dimension of the annular gap (Loganathan, et al., 1998)	12
Figure 6 Selection of the conditioning agent based on the grain size distribution (DAUB, 2016)	14
Figure 7 Contribution of the overall ground settlement.....	16
Figure 8 Shape of the settlement trough (Mair, et al., 1997)	21
Figure 9 Twin tunnels layouts (Hunt, 2005).....	30
Figure 10 Limbs of the settlement trough (Hunt, 2005)	32
Figure 11 Damage control parameters (Guglielmetti, et al., 2007).....	36
Figure 12 Deep beam model (Burland, et al., 1974)	39
Figure 13 Sign of the horizontal displacement	41
Figure 14 Settlement under a reinforced concrete building	43
Figure 15 Risk matrix.....	46
Figure 16 Longitudinal section of the studied area.....	47
Figure 17 Stratigraphy of the studied area	48
Figure 18 Dimensions of the model.....	52
Figure 19 Material menu	54
Figure 20 Property menu	54
Figure 21 Size Control menu	55
Figure 22 Mesh menu	56
Figure 23 Rename menu	56
Figure 24 Change Property menu.....	57
Figure 25 Scheme used for the equivalent parameter computation	59

Figure 26 Anagnostou & Covari nomograms	60
Figure 27 Names of the mesh sets for the tunnel.....	63
Figure 28 Names of the mesh set for the soils.....	63
Figure 29 Stage Wizard definition	64
Figure 30 Borehole definition.....	66
Figure 31 Interfaces.....	66
Figure 32 Horizontal configuration.....	67
Figure 33 Offset configuration	68
Figure 34 Piggyback configuration.....	68
Figure 35 Mesh generation	69
Figure 36 Stage Construction	72
Figure 37 Vertical displacements upper first construction sequence	74
Figure 38 Vertical displacements bottom first construction sequence	74
Figure 39 Comparison of the construction sequences: vertical settlement	75
Figure 40 Layouts of the twin tunnels	76
Figure 41 Results worst arrangement VL=0.5%	78
Figure 42 Results worst arrangement VL=1.0%	78
Figure 43 Piggyback upper first: surface displacements	79
Figure 44 Piggyback upper first: vertical displacements	80
Figure 45 Plaxis 2D model for piggyback layout	80
Figure 46 Comparison of the construction sequences: volume loss	84
Figure 47 Comparison of the construction sequences: maximum vertical displacement.....	84
Figure 48 Comparison of the construction sequences: maximum angular distortion	85
Figure 49 Position and geometrical characteristics of the building	86
Figure 50 Building foundation settlement	87

Figure 51 Subsurface settlement.....	88
Figure 52 Category of damage - upper first.....	89
Figure 53 Category of damage - bottom first.....	90
Figure 54 Risk matrix related to the studied project	91
Figure 55 Risk related to the maximum vertical deformation	91
Figure 56 Risk related to the maximum angular distortion.....	92
Figure 57 Risk related to the total deformation	92

TABLE INDEX

Table 1 Vulnerability index.....	38
Table 2 Damage classification (Burland, et al., 1977)	42
Table 3 Damage classification (Rankin, 1988).....	43
Table 4 New Burland damage classification (Chiriotti, et al., 2000).....	44
Table 5 New Rankin damage classification (Chiriotti, et al., 2000).....	45
Table 6 Geomechanical parameters of the layers	49
Table 7 Mechanical parameters of the structural elements	51
Table 8 Studied chainage and relative tunnels coordinates.....	51
Table 9 Equivalent parameter for the pressure calculation.....	59
Table 10 Support pressures for twin tunnels.....	71
Table 11 Deconfinement values for single tunnels.....	77
Table 12 Outputs for the two different construction sequence.....	82
Table 13 Building characteristics	86
Table 14 Example of damage class evaluation procedure	88